Robot-Assisted Transcranial Magnetic Stimulation (Robo-TMS): A Review

Wenzhi Bai, Andrew Weightman, Rory J O'Connor, Zhengtao Ding, *Senior Member, IEEE*, Mingming Zhang, *Senior Member, IEEE*, Sheng Quan Xie, *Fellow, IEEE*, and Zhenhong Li, *Senior Member, IEEE*

***Abstract*— Transcranial magnetic stimulation (TMS) is a non-invasive and safe brain stimulation procedure with growing applications in clinical treatments and neuroscience research. However, achieving precise stimulation over prolonged sessions poses significant challenges. By integrating advanced robotics with conventional TMS, robot-assisted TMS (Robo-TMS) has emerged as a promising solution to enhance efficacy and streamline procedures. Despite growing interest, a comprehensive review from an engineering perspective has been notably absent. This paper systematically examines four critical aspects of Robo-TMS: hardware and integration; calibration and registration; neuronavigation systems; and control systems. We review state-of-the-art technologies in each area, identify current limitations, and propose future research directions. Our findings suggest that broader clinical adoption of Robo-TMS is currently limited by unverified clinical applicability, high operational complexity, and substantial implementation costs. Emerging technologies—including marker-less tracking, non-rigid registration, learning-based electric field (E-field) modelling, individualised magnetic resonance imaging (MRI) generation, robot-assisted multi-locus TMS (Robo-mTMS), and automated calibration and registration—present promising pathways to address these challenges.**

***Index Terms*— Transcranial magnetic stimulation, non-invasive brain stimulation, medical robots, image-guided robotic systems, registration, neuronavigation, optical tracking systems.**

Received 10 April 2025; revised 2 June 2025; accepted 30 June 2025. Date of publication 4 July 2025; date of current version 10 July 2025. This work was supported in part by the Engineering and Physical Sciences Research Council (EPSRC) of U.K. under Grant EP/V057782/2, in part by the Royal Society of U.K. under Grant IEC/NSFC/233142, and in part by the Medical Research Council of U.K. under Grant IAA-549. *(Corresponding author: Zhenhong Li.)*

Wenzhi Bai, Zhengtao Ding, and Zhenhong Li are with the Department of Electrical and Electronic Engineering, University of Manchester, M13 9PL Manchester, U.K. (e-mail: wenzhi.bai@manchester.ac.uk; zhengtao.ding@manchester.ac.uk; zhenhong.li@manchester.ac.uk).

Andrew Weightman is with the Department of Mechanical and Aerospace Engineering, University of Manchester, M13 9PL Manchester, U.K. (e-mail: andrew.weightman@manchester.ac.uk).

Rory J O'Connor is with the School of Medicine, University of Leeds, LS2 9JT Leeds, U.K. (e-mail: R.J.O'Connor@leeds.ac.uk).

Mingming Zhang is with the Department of Biomedical Engineering, Southern University of Science and Technology, Shenzhen 518055, China (e-mail: zhangmm@sustech.edu.cn).

Sheng Quan Xie is with the School of Electronic and Electrical Engineering, University of Leeds, LS2 9JT Leeds, U.K. (e-mail: S.Q.Xie@leeds.ac.uk).

Digital Object Identifier 10.1109/TNSRE.2025.3585651

I. Introduction

TRANSCRANIAL magnetic stimulation (TMS) is a non-invasive and safe brain stimulation procedure first introduced in 1985 [1]. It utilises a time-varying electromagnetic field generated by coils to induce an electric current in targeted brain regions [2], [3], [4]. As neurogenic diseases and mental disorders remain leading causes of disability and continue to pose a significant global health burden [5], there is a growing demand for effective diagnostic and therapeutic tools. Leveraging its neurostimulation and neuromodulation capabilities, TMS has been extensively explored for diagnosing and treating various neurogenic diseases and mental disorders [6], [7], [8], as well as for brain mapping research [9], [10], [11], [12]. Since TMS does not require active subject participation, it can be effectively performed on individuals who are paralysed, sedated, or uncooperative [13]. Following its initial approval by the U.S. Food and Drug Administration (FDA) in 2008, TMS has seen growing adoption in neurosurgery planning and treating depression, obsessive-compulsive disorder (OCD), migraines, and smoking cessation especially when standard treatments have proven ineffective [14], [15].

In conventional TMS, clinicians cannot directly visualise the stimulation spot beneath the scalp, and even the corresponding location on the subject's head is often obscured by the stimulation coil. Maintaining precise targeting throughout prolonged sessions is further complicated by the need to manually hold the coil. To address these challenges, advanced robotics innovations have been integrated into conventional TMS to enhance clinical outcomes. These advancements include neuronavigation systems for accurate stimulation targeting, electric field (E-field) modelling for the estimation of induced E-field distribution, optical tracking systems for subject's head movements compensation, and robot arms for stable and precise coil placement. Reflecting these new capabilities, the terminology used to describe these procedures has evolved: TMS enhanced with neuronavigation systems is often referred to as navigated TMS (nTMS) [16]; automated systems that incorporate robot arms are termed robotic TMS, robotised TMS, robot-assisted TMS (RA-TMS),

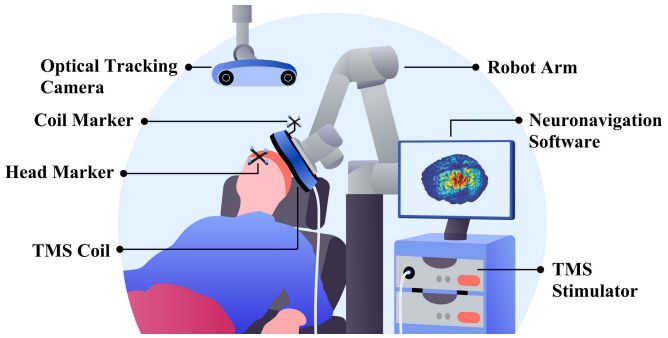

Fig. 1. A typical application scenario of Robo-TMS. The subject lies in a chair with a head marker attached. An optical tracking camera monitors head and coil markers to guide the robot arm in compensating for head movements, maintaining a consistent coil-to-head transformation for accurate stimulation. The TMS stimulator generates current pulses into the TMS coil, and the resulting induced E-field within the subject's head is visualised by the neuronavigation software on the monitor.

or robot-assisted image-guided TMS (RI-TMS) [17]. To ensure clarity and consistency, we adopt the term robot-assisted TMS (Robo-TMS) to describe the integrated system illustrated in Fig. 1.

Recent literature on PubMed indicates a growing interest among medical researchers in more advanced TMS devices to meet evolving clinical needs. However, comprehensive reviews on Robo-TMS, particularly from an engineering perspective, are absent. Existing reviews primarily focus on the fundamental aspects of TMS [3], [13], [18] and its clinical applications [7], [8], [9]. Some reviews emphasise the importance of neuronavigation systems and the necessity for high accuracy [19], [20], [21], while others delve into specific aspects like E-field modelling [22], [23], brain mapping [24], and accuracy comparisons across different systems [25], [26], [27], [28]. Although early insights into Robo-TMS are provided by a book [29] and a doctoral thesis [30] over a decade ago, the rapid advancements in robotics underscore the need for a comprehensive review that introduces emerging engineering tools for addressing current challenges in TMS practice and informs the development of technology that aligns with clinical requirements.

This review focuses on the core technologies and components of Robo-TMS, while omitting elements that have been widely discussed in conventional TMS, such as pulse waveform, cooling, power supply and etc. The main objectives are

1) to identify the status and challenges in four critical aspects: hardware and integration, calibration and registration, neuronavigation systems, and control systems;
2) to bridge the gap between the medical and engineering perspectives, providing a comprehensive understanding of Robo-TMS;
3) to propose directions for further research and development by discussing how to potentially enhance clinical outcomes and reduce operational costs.

To the best of our knowledge, this is the first review to comprehensively survey the status and challenges of Robo-TMS from an engineering perspective. We hope it can foster collaboration among clinicians, engineers and researchers, ultimately driving future advancements in the field.

II. Hardware and Integration

A. System Setup

Manually holding the coil for prolonged TMS procedures not only exhausts clinicians but also leads to inaccuracies caused by fatigue, affecting stimulation efficacy. While mechanical holders offer some stability [39], they are unable to compensate for unexpected head movements. Compromised solutions, such as instructing subjects to remain still or employing head restraints, often cause discomfort and stress. Robo-TMS, which integrates neuronavigation with a robot arm to ensure accurate coil targeting and precise coil placement, has been developed aiming to enhance both comfort and the overall efficacy of stimulation. In 2000, the first Robo-TMS system was developed by mounting a TMS coil onto the neurosurgical robot NeuroMate, a five-joint serial robot [40]. This system achieves precise coil placement with an accuracy of approximately 2mm [41]. However, due to the lack of head-tracking capability, it requires subjects to maintain a stationary head position during procedures.

Subsequent Robo-TMS systems can be broadly categorised into two types: industrial robot-based systems, valued for their adaptability and accessibility; and specialised robot-based systems, tailored to clinical safety and efficacy requirements with enhanced integration. A typical industrial robot-based system is first introduced by adapting a standard six-joint industrial robot and integrating it with an optical tracking system for automated neuronavigation [30], [42]. Later advancements incorporate force sensors for collision avoidance and safe coil-to-head contact [29]. Other industrial robot-based systems employ similar configurations [43], [44], including a parallel industrial robot-based system designed to enhance stiffness and reduce moving mass, enabling faster and more precise coil placement [45]. In parallel, specialised robot-based systems also incorporate the optical tracking system and force sensors but differ by employing customised designs to stabilise the dynamic coil cable and constrain coil movement tangentially to the subject's head, thereby better meeting clinical requirements for safety and efficacy [31], [35], [46], [47]. Both types of systems underscored the importance of integrating force or torque sensors to adjust contact forces dynamically [48], ensuring the stimulation coil maintained optimal proximity to the scalp—a key factor in achieving effective stimulation [49]. A comparison of typical TMS system configurations and their performance is provided in TABLE I.

Building on these typical systems, innovations have continued to refine Robo-TMS. To address tracking loss caused by robot occlusion, some systems mount cameras directly onto the robot's end-effector, ensuring continuous visual feedback during procedures [50]. Teleoperated haptic-enabled Robo-TMS systems are developed to facilitate remote TMS treatments, providing significant benefits for rural healthcare delivery [51]. Recent advancements have also focused on marker-less tracking, eliminating the need for head and coil markers [52], [53]. This method simplifies registration processes, minimises manual errors, shortens treatment times,

TABLE I
THE COMPARISON OF TYPICAL TMS SYSTEMS

	Conventional TMS System	Industrial Robot-based Robo-TMS System	Specialised Robot-based Robo-TMS System
Holders	Passive Mechanical Holder	Active Industrial Robot Arm	Active Specialised Robot Arm
Force / Torque Sensors	None	Required	Required
Optical Tracking	Optional	Required	Required
E-field Modelling	Optional	Recommended	Recommended
Accuracy*	~ 6mm/ $\sim 3^\circ$ [31]–[33]	~ 2mm/ $\sim 1.5^\circ$ [31]–[33]	~ 2mm/ $\sim 1.5^\circ$ [31]–[33]
Contact Force*	$6-10$N [34]	~ 2.5N [32], [35]	~ 2.5N [32], [35]
Examples	 Magstim^{TM} Horizon Lite [36]	 Axilum Robotics^{TM} TMS-Cobot [37]	 Yiruide^{TM} Mag-aim [38]

* Accuracy and contact force listed in the table are for specific commercial systems and experimental prototypes.

and consequently enhances the overall experience for both clinicians and subjects. Additionally, novel multi-locus TMS (mTMS) systems utilise coil arrays to produce spatially controlled magnetic fields [54], [55]. By integrating robotic movements with spatially controlled magnetic fields, robot-assisted mTMS (Robo-mTMS) achieves rapid and accurate targeting [56], [57].

Currently, four commercial Robo-TMS systems lead the market: Axilum Robotics' TMS-Cobot and ANT's Smart-move (industrial robot-based systems); Axilum Robotics' TMS-Robot and Yiruide's Mag-aim (specialised robot-based systems). Notably, Axilum Robotics' TMS-Cobot is the first Robo-TMS system to receive clearance from the U.S. FDA for clinical use. Although Robo-TMS offers advantages over conventional TMS, its clinical adoption remains in the early stages and continued developments are essential to fully realise its potential.

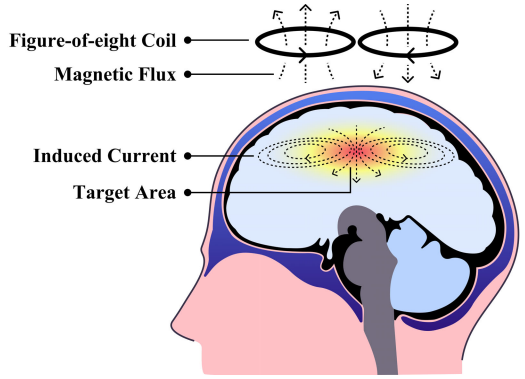

Fig. 2. The principle of TMS. TMS operates on the principle of electromagnetic induction (Faraday's law of induction). A rapidly changing current passing through the coil generates a brief magnetic field pulse, which induces electric currents in the targeted brain region. The distribution of the induced E-field is influenced by the coil design, its placement on the scalp, and the intensity of the applied current.

B. Coil Design

The TMS uses a high-voltage power supply to charge capacitors, which are then rapidly discharged into the TMS coil. This process generates a brief magnetic field pulse, delivered via electromagnetic coils placed on the subject's scalp. The pulse induces electric currents in the underlying cortical tissue, which can stimulate neurons when these currents exceed a threshold [58]. This capability allows TMS to stimulate specific brain regions, potentially controlling neural activation. The principle of TMS is shown in Fig. 2.

The design of the TMS coil, including its shape, size, and number of winding turns, is crucial for stimulation safety and efficacy. The coil's configuration affects not only how the E-field is distributed within the brain but also its intensity and pulse width. The primary objective of coil design is to enable targeted brain stimulation while minimizing unintended activation of surrounding brain regions [3], [6].

1) Standard Coils: The circular coil or round coil is the most basic coil design, generating an annular E-field. Circular coils, typically 9cm in diameter, penetrate relatively deep, inducing currents over broad brain regions. This non-focal stimulation uniformly activates all regions beneath the coil's annulus at peak current densities. As a result, effective stimulation requires placing the annulus, rather than the coil's centre, over the target cortex [2], [59].

The figure-of-eight coil, first introduced in 1988 [60] and also known as a double or butterfly coil, consists of two adjacent circular coils with opposing currents. This design generates the highest current density directly beneath the coil intersection, where the E-field aligns parallel to the wires at the centre. Consequently, focal stimulation is achieved by placing the coil's centre over the target, concentrating the current in a central region with a density two to three times higher than at the edges. This focality makes the figure-of-eight coil ideal for precise cortical stimulation in both research and clinical applications [2], [59], [61].

2) Coils for Deep TMS: Standard TMS coils, mainly stimulate superficial cortical regions, as their E-field intensity decreases rapidly with depth [62]. Consequently, reaching deeper brain regions necessitates substantially higher intensities, which may exceed the capabilities of standard coils and pose safety concerns such as discomfort and side effects. To address these limitations, deep TMS (dTMS) coils have been developed with optimised E-field distribution that has higher intensity at deeper regions while minimising excess stimulation at the cortical surface by reducing E-field decay [63]. This innovation is particularly valuable for treatments requiring direct stimulation of deep neural pathways. Below are some common dTMS coil designs:

a) Double-cone coils: The double-cone coil, also known as an angled butterfly coil, is an enlarged version of the figure-of-eight coil. Its two circular windings are angled towards the subject's head, enhancing the magnetic field strength and electrical efficiency at greater depths. This coil penetrates deeper into the brain but is less focal than the standard figure-of-eight coil, making it suitable for stimulating regions 3−4cm deep, such as the primary motor region of the leg [59].

b) H-coils: The H-coil, or termed Hesed coil, is designed to induce a deeper E-field than figure-of-eight coils, albeit with reduced focality [49]. The H-coil features a complex winding pattern and larger dimensions, with elements strategically placed around the target brain region to generate a summation of the E-field at a depth of 4 − 6cm. This design allows for deeper brain stimulation without excessively stimulating the cortical surface [59], [63], [64].

c) Halo circular assembly coils: The halo circular assembly coil (HCA-coil) is a large circular coil designed to be placed around the head, providing sub-threshold E-field stimulation in deep brain tissues. It can be used in conjunction with a conventional circular coil positioned at the top of the head. This design allows for more flexible and deeper brain stimulation than standard circular coils, with additional coaxial circular coils developed to reduce E-field intensity in superficial cortical regions [59].

d) Helmet coils: The helmet coil, a dTMS coil with customised geometry, is designed using continuous current density inverse boundary element method (IBEM) to optimise depth control and minimise power dissipation. Its subject-specific design, tailored to the shape of the subject's head, enables focal stimulation in regions such as the prefrontal cortex and right temporal lobe. According to [65], helmet coils can increase stimulation depth by over 15% compared to H-coils with similar focality.

3) Coils for Multi-Locus TMS: Conventional TMS coils stimulate a fixed location directly beneath the coil, requiring physical movement to target different brain regions. This physical movement is slow and limits applications like feedback-controlled stimulation, where rapid adjustments are necessary. To overcome these limitations, a 2-coil mTMS system has been developed, enabling electronic targeting of nearby cortical regions along a 30mm line segment without moving the coil [54]. Further advancements include a 5-coil mTMS system that allows for adjusting the location and orientation of the E-field maximum within a 30mm diameter cortical region [55]. Design optimisation of mTMS has also been investigated to address the manufacturing challenges of mTMS coils, such as excessive winding density [66]. Although mTMS coils enable faster and more complex stimulation patterns, targeting multiple brain regions with varying E-field directions, timings, and intensities, the stimulation region of mTMS is still limited due to manufacturing challenges.

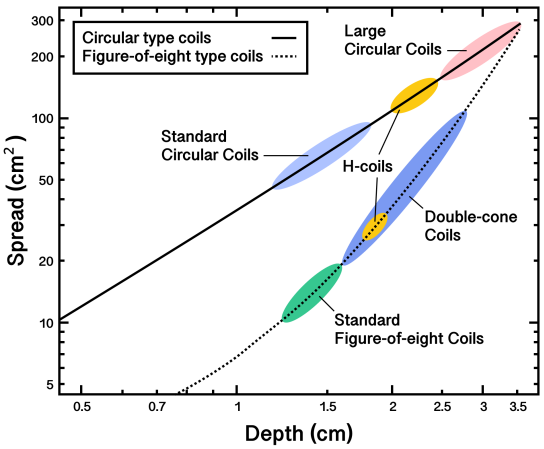

Fig. 3. The depth-focality trade-off in TMS coil design. The depth is quantified by $d_{1/2}$, and the focality is quantified by the spread $S_{1/2}$. For any type of coils, deeper stimulation is accompanied by increased spread, indicating reduced focality [59], [61].

4) Depth-Focality Trade-off: In TMS coil design, there is a fundamental trade-off between stimulation depth and focality as shown in Fig. 3. Larger coils penetrate deeper into the brain but at the cost of reduced focality, stimulating larger regions of the brain surface. Conversely, coils designed for focal surface stimulation experience rapid E-field decay at greater depths, limiting their efficacy in deeper regions [62]. Simulations of 50 coil designs highlight this depth-focality trade-off, illustrating the challenge of achieving both deep penetration and precise targeting in TMS [59].

This trade-off can be quantified by metrics such as E_{max} (the maximum E-field strength), $d_{1/2}$ (the depth at which the E-field drops to half of E_{max}), and $S_{1/2} = \frac{V_{1/2}}{d_{1/2}}$ (a focality measure), where $V_{1/2}$ indicates the volume beneath the cortical surface in which the E-field exceeds $\frac{1}{2}E_{max}$, with smaller $S_{1/2}$ values indicating better focality [59], [67], [68]. Based on quantitative metrics, multi-objective optimisation algorithms can be used to generate the computational design of TMS coils that balance focality, depth, and energy efficiency, reaching specific depths without exceeding predefined E-field strength limits [69]. A similar trade-off also applies to mTMS. By examining the interplay among coil number, focality, and the cortical region over which the E-field peak can be controlled, researchers have shown that expanding the controllable region while maintaining the same number of coils necessitates a compromise in E-field focality [70].

III. Calibration and Registration

Calibration and registration are essential to ensure accurate targeting and efficient stimulation of brain regions by establishing the initial settings and subject-specific configurations, including workspace calibration, registration and

stimulation intensity calibration. These processes align the robot's workspace, optical tracking systems, and the subject's anatomy, while also adapting the equipment's parameters to individual characteristics.

A. Workspace Calibration

Workspace calibration in Robo-TMS synchronises the coordinate systems of the camera and the robot, enabling accurate transformation of visual information into robot movements. Without proper calibration, the robot cannot accurately interpret the target within its workspace, leading to operational inaccuracies.

In robotics, calibrating the spatial relations between a robot arm and a camera is a well-established problem, commonly known as hand-eye or robot-world calibration. The calibration can be divided into two categories based on the configurations of the camera-robot system: eye-to-hand and eye-in-hand. As a natural extension of conventional TMS systems where the coil is handheld, most Robo-TMS systems [32], [53], [71], [72] adopt the same eye-to-hand configuration to keep the coil-holding device lightweight and mechanically simple. In this setup, the camera is fixed in the workspace and operates independently of the robot arm's movements. More recent Robo-TMS systems [50] explore the eye-in-hand configuration, where the camera is mounted on the end-effector and moves with the robot arm. This setup ensures that the camera's line of sight remains unobstructed by the robot throughout the procedure. However, it is generally limited to marker-based tracking systems, as mounting the camera on the end-effector makes it difficult to capture facial features, which are commonly used in marker-less tracking.

Regardless of the configuration, the core concept of hand-eye calibration is to ensure that the relative motion observed by both the robot (hand) and the camera (eye) is consistent, allowing the rigid transformation between different components to be accurately estimated through multiple observations. Mathematically, the common eye-to-hand calibration problem can be expressed by the equation shown below.

$$\mathbf{MX} = \mathbf{YN} \tag{1}$$

where all matrices are 4×4 homogeneous transformations in special Euclidean group $SE(3)$. Here, $\mathbf{M}$ represents the transformation between the robot's end-effector frame and the robot's base frame, $\mathbf{N}$ represents the transformation between the coil frame and the camera's base frame, and $\mathbf{X}$ and $\mathbf{Y}$ are the unknown transformations between the robot's end-effector and coil frames, and the robot's base and camera's base frames, respectively.

Building on standard calibration techniques, the method described in [32] is optimised for Robo-TMS by accounting for the robot's specific workspace during treatments, characterised as a spherical shell around the subject's head. Tested across three calibration algorithms—SGO [73], QR24 [74], and QUAT [75]—it reduces positional error by 34% and orientation error by 19%. Additionally, a method employs an optical tracking system to independently measure coil geometry and compute the required transformation with high accuracy [76].

B. Registration

After workspace calibration, the robot arm can accurately interpret and locate targets from the optical tracking system within its workspace. However, to stimulate the target tissue effectively, individual factors—such as the size and shape of the head and brain, the distance between the stimulating coil and the target tissue, as well as the location and orientation of anatomical structures—must be defined for each subject [13], [77]. Consequently, an individual or individualised magnetic resonance imaging (MRI) is typically required to represent the subject's static neuroanatomy for alignment. In fact, spatial and temporal alignment are critical in any multi-source system. In Robo-TMS, registration refers to aligning the MRI of the subject's neuroanatomy with the physical head in the workspace, a prerequisite for neuronavigation [78]. Once registration is complete, the subject's neuroanatomy can also be represented in the robot's workspace, enabling Robo-TMS to visualise brain structures despite their location within the physical head. This alignment facilitates accurate stimulation within the most intricate organ in the human body.

A comprehensive analysis reveals that the registration method is a major contributor to the level of error in neuronavigation [79]. In Robo-TMS, two main types of registration methods are commonly used: landmark-based registration and surface-based registration. Landmark-based registration involves manually selecting at least three corresponding points on the MRI and the subject's head, but it generally offers lower accuracy and precision than surface-based methods due to limited landmarks [80]. Common landmarks include the nasion (bridge of the nose), the left and right pre-auricular points, and occasionally the tip of the nose. However, the manual selection of landmarks leads to registration errors. In [79], mean errors of 2.9mm/1.1° for accuracy and 1.4mm/0.6° for precision were reported, with larger errors observed in posterior regions of the head [81], [82].

By contrast, surface-based registration, which starts with landmark-based alignment followed by digitising points on the scalp and matching them to a scalp mesh derived from the MRI, significantly reduces human-induced errors. This method achieves mean errors of 1.0mm/0.7° for accuracy and 0.6mm/0.4° for precision [79]. However, challenges remain, particularly with the use of 3D stylus digitisers, which require manual manipulation and longer measurement times. As highlighted by [20], the time required for registration is a critical factor in operating room efficiency, as clinicians must wait for registration to be completed before continuing the procedure. During the procedure, any fiducial marker shift necessitates re-registration, further delaying the process. To address these limitations, advanced surface-based 3D digitisation techniques, such as 3D laser scanning [83] and photogrammetry-based systems [84], have been proposed. These methods enhance accuracy while streamlining the registration process.

In addition, registration can also be performed using either rigid or non-rigid methods. Rigid registration considers only translation and rotation, ignoring the complex spatial deformations inherent to soft tissues. While rigid methods currently dominate Robo-TMS due to the skull's rigid structure, they are

less suitable for aligning soft tissue regions such as the face and brain, where non-rigid deformation is common. Non-rigid registration methods offer the potential to improve alignment accuracy in these areas by modelling such deformations. However, they remain relatively immature and face challenges including sensitivity to noise, outliers, varying deformation levels, and incomplete data [85]. These limitations reduce robustness and increase computational complexity. Nevertheless, as non-rigid methods mature, they are expected to further improve registration accuracy and precision in Robo-TMS applications [19], [78], [86].

C. Stimulation Intensity Calibration

The TMS treatment begins with a mandatory step to determine the appropriate stimulation intensity for the target region [6], [8], as this depends on the subject's unique neuroanatomy and is essential for personalised treatment. Typically, the motor threshold (MT), defined as the minimum stimulation intensity that corresponds to a 50% probability of eliciting a motor response, serves as a reference for calibrating stimulation intensity at other cortical targets. To establish the MT, clinicians first search within the primary motor cortex (M1) using a clinically guided starting intensity to locate the motor hotspot, where stimulation could evoke responses in a target muscle, commonly the first dorsal interosseous or abductor pollicis brevis of the dominant hand. Once the motor hotspot is identified, the stimulation intensity is gradually adjusted to determine the resting or active MT by recording the muscle responses evoked by stimulation. Subsequent stimulation intensities for the target region are then expressed as a percentage of the individual's MT, in accordance with safety guidelines and to standardise stimulation [4], [87].

While early methods efficiently automate MT estimation [88], clinicians still need to first manually identify the hotspot, introducing variability between clinicians. To address this, the first automated hotspot localisation method based on MTs mapping has been introduced [89]. Building on this, AutoHS—a probabilistic Bayesian model—has been developed to automate hotspot localisation, offering improved reproducibility, speed, and reliability compared to earlier methods [90]. By integrating AutoHS with Robo-TMS and automated MT estimation, the first fully automated setup procedure for Robo-TMS has been proposed, aiming to reduce inter-subject variability and minimise setup time [90].

However, these automated stimulation intensity calibration methods require a large number of motor evoked potential (MEP) measurements and operate with a fixed stimulation orientation. Furthermore, these methods heavily rely on sparse grids between coil positions, potentially limiting accuracy. To overcome these limitations, recent studies [91], [92] introduce algorithms supported by mTMS, designed to automatically optimise stimulation parameters, location, and orientation to elicit the largest MEPs.

IV. Neuronavigation Systems

The neuronavigation system utilises optical tracking and E-field modelling, alongside neuroanatomical data, to provide real-time guidance to clinicians during procedures. This system serves as a critical component of Robo-TMS. As discussed in Section III, workspace calibration establishes the transformation between the coordinate systems of the optical tracking camera, the coil, and the robot arm, while registration establishes the relationship between the image of an individual's brain anatomy and their physical head. However, compared to calibration and registration that occur during the initial setup, the neuronavigation system is essential for determining the real-time pose relationship between the head and the coil within the optical tracking camera's coordinate system, as well as the induced E-field based on this relative pose during the procedure. An overview of the neuronavigation system for Robo-TMS is shown in Fig. 4. The U.S. National Institute of Mental Health (NIMH) recommends neuronavigation on an individual basis in all TMS applications to standardise coil localisation and account for individual differences in the delivered dose, thereby improving the rigour and repeatability of non-invasive brain stimulation studies [6].

A. Optical Tracking

As discussed in Section II-B, the pose of the coil above the scalp significantly influences both the distribution and intensity of the induced E-field within the target stimulation region [93]. Tracking devices, a crucial component of the neuronavigation system [94], enable accurate and real-time monitoring of the coil's pose relative to the subject's head. Conventional neurosurgical tracking methods include invasive frame-based systems, which secure pins to the subject's skull before brain scanning and later attach rigid frames for navigation, and non-invasive electromagnetic tracking, which localises sensors within a magnetic field. While both methods offer high accuracy, they are unsuitable for Robo-TMS due to their operational inconvenience and susceptibility to interference. In contrast, optical-based frame-less stereotactic systems, also known as optical tracking systems, are widely employed in TMS, relying on markers attached to the subject's head and the coil to track the coil's pose relative to the head [18].

Optical tracking systems can be classified into two types based on the light source: active and passive optical tracking. The key difference between them is whether the marker emits light. In active optical tracking, powered markers with integrated light-emitting diodes (LEDs) emit infrared (IR) light, which is tracked by IR cameras to determine the pose of the instruments. This system is more resistant to ambient light interference, making detection easier. However, the markers require power, which introduces additional weight and complexity due to the need for batteries or wires. In contrast, passive optical tracking uses reflective markers attached to the subject or instruments. The optical camera detects light reflected from these markers to determine their pose. Since passive markers don't require power, they enable simpler setups and are widely used.

Markers, also referred to as trackers, work alongside optical tracking cameras to form an optical tracking system. They are generally divided into three categories based on their form: array-based markers, pattern-based markers, and natural features (marker-less). Array-based markers, the most common in Robo-TMS, consist of three or more reflective markers arranged in a known geometric configuration [32], [44]. Their pose is captured by two or more cameras positioned

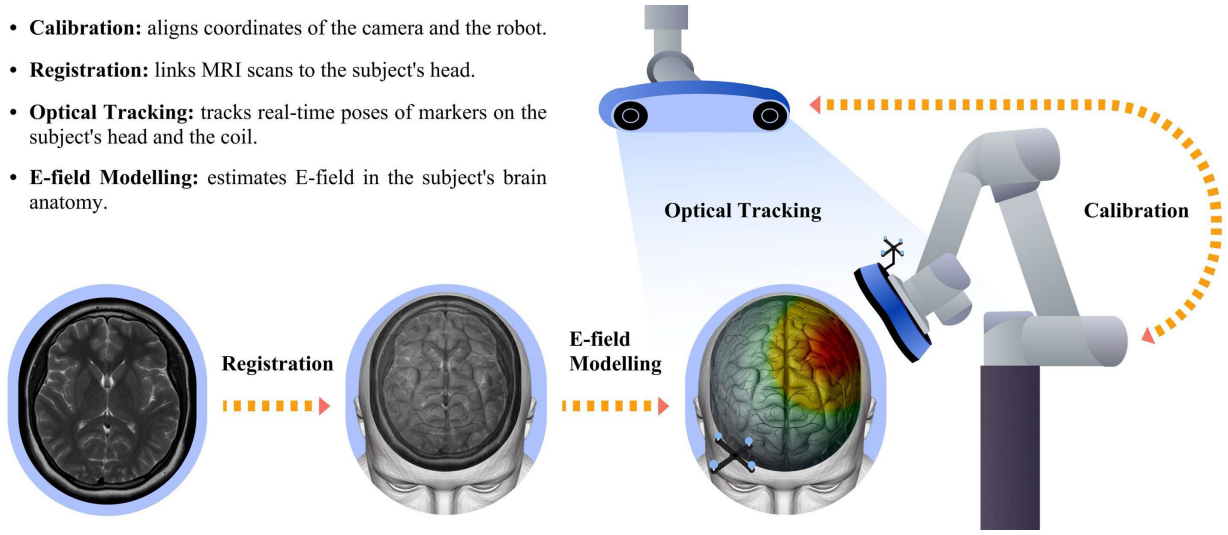

Fig. 4. The neuronavigation system for Robo-TMS. The optical tracking camera continuously monitors the real-time poses of markers on the coil and the subject's forehead, enabling accurate tracking of both the coil and head poses. Through calibration, these poses are transformed from the camera's base frame to the robot's base frame for robot control, providing an accurate coil pose relative to the subject's head. With individual MRIs registered to the subject's physical head, E-field modelling can then visualise the resulting E-field distribution within the brain.

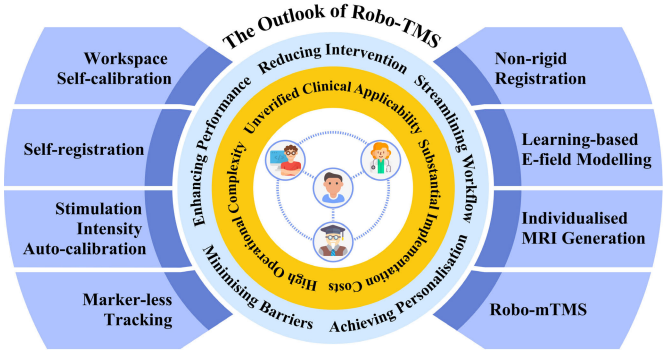

Fig. 5. The outlook of Robo-TMS. Advancements in Robo-TMS have been driven by collaborative efforts among clinicians, engineers, and researchers. However, the challenges highlighted in the yellow ring remain unresolved, hindering progress towards the future directions outlined in the light blue ring. Promising solutions have begun to emerge, requiring further exploration to realise their full potential.

at different angles, which triangulate the marker's position. Pattern-based markers, on the other hand, use predefined, high-contrast patterns—such as AprilTags [95] and ArUco markers [96]—printed on flat surfaces [97], [98]. Cameras detect and identify these unique patterns from a preloaded library and calculate the marker's spatial pose. These markers are easier and cheaper to produce and manage and can operate under normal lighting conditions without relying on IR light. However, both array-based and pattern-based systems require the attachment and management of external markers. Marker-less tracking, which relies on detecting natural features from the subject's head and face, reduces setup time and eliminates the risk of marker detachment or movement during procedures [52], [53]. However, it is less robust compared to marker-based systems, primarily due to its relative immaturity and the challenges in consistently identifying natural surface features.

Conventionally, the optical camera is positioned outside the robot arm to maximise its field of view (FOV) for tracking the head and coil. However, this setup can result in tracking loss if the robot arm obstructs the camera's line of sight during movement. To address this issue, an inside-out tracking method, where a portable camera is mounted on the robot's end-effector, has been proposed [50]. This method ensures that the camera maintains an unobstructed view of the head and coil throughout the robot's motion.

B. E-Field Modelling

Unlike neuronavigation systems for neurosurgery, which primarily track instrument poses relative to the brain, Robo-TMS requires both real-time tracking of the coil pose and estimation of induced E-field distribution to assess the electric currents that stimulate target neurons. The E-field modelling is essential for understanding TMS effects on neural tissue and tailoring stimulation protocols to specific brain regions or individuals, as TMS needs to properly engage disease-related pathways to improve clinical outcome [99]. Accurate and real-time E-field modelling relies on two factors: realistic head models and robust E-field modelling solvers.

1) Realistic Head Models: Early head models in TMS rely on simplified geometries as standard templates, such as infinite half-planes or perfect spheres fitted locally or globally to the subject's head [100], [101]. However, comparisons with more realistic head models [18], [102] have demonstrated that these simplified models lack accuracy due to the omission of structural details and tissue conductivity [79], [103]. Modern head models, such as those developed by [104], offer improved structural detail, resolution, and tissue conductivity, setting a new standard.

Despite improvements in standard head models, research highlights that individual anatomical variations significantly affect E-field distribution, emphasising the need for personalised stimulation protocols [105], [106]. In response,

toolboxes have been developed to automate the creation of individualised head models from MRI [107], [108], [109]. These early toolboxes typically segment five major head tissues and assign different tissues with their conductivity for E-field modelling [109], [110], [111]. Further results in [112] demonstrate that increasing the number of segmented tissues to fifteen from MRI significantly improves accuracy, reducing the relative error in E-field estimation. This advancement allows for more precise and individualised E-field modelling.

2) E-Field Modelling Solvers: E-field modelling solvers are computational tools used to estimate the E-field induced by TMS within the brain. These solvers estimate the E-field distribution based on coil placement and current parameters, along with detailed head models that represent tissue geometry and conductivity. While high-resolution head models are crucial for accurate E-field estimations in Robo-TMS, they are often computationally expensive. To achieve real-time E-field modelling, essential for TMS treatment involving moving coils, the trade-off between computational speed and accuracy has to be considered [113]. Broadly, E-field solvers can be categorised into two main types: physics-based solvers and learning-based solvers.

Basic physics-based solvers assume the E-field peak occurs where the coil normally intersects the cortex [114], enable real-time estimation but are inaccurate, particularly with non-tangential coil placements [115]. More sophisticated physics-based solvers typically employ methods like finite element method (FEM), boundary element method (BEM), and finite difference method (FDM), which numerically solve Maxwell's equations to estimate the E-field induced by time-varying magnetic fields.

FEM is widely used due to its ability to model complex geometries and varying material properties by dividing the head model into finite elements, such as tetrahedrons, and calculating electromagnetic fields locally. It is ideal for heterogeneous models but is computationally intensive due to the large number of elements required for high-resolution simulations [106], [116], [117], [118], [119]. BEM, on the other hand, simplifies computations by discretising only the model's surfaces. It is particularly effective when the head can be approximated by layered tissues with homogeneous conductivity [120], [121], [122], [123], [124]. FDM employs a structured grid to solve equations through finite difference approximations. While easier to implement due to structured grids, it is less flexible for complex geometries and better suited to simplified or idealised head models [125], [126], [127].

Physics-based solvers are widely adopted in E-field modelling software. Commercial software—such as COMSOL Multiphysics [128], ANSYS Maxwell 3D [104], [129], Sim4Life [130], and SEMCAD X [131]—are not specifically developed for TMS E-field modelling, which limits their suitability for real-time Robo-TMS applications. In contrast, open-source software like SimNIBS [107], [111], [132], [133] and ROAST [109], [134] are well-maintained and facilitate visualisation of the E-field distribution in the brain. Neural Navigator, a clinical software designed for nTMS [135], is compatible with various TMS devices and has received FDA clearance for clinical use.

In addition to these physics-based methods, learning-based E-field estimation has emerged as a promising solution to reduce computation times in real-time modelling. These models leverage the computational power of graphics processing units (GPUs) to learn and approximate complex relationships between coil placement, current parameters, head anatomy, and the resulting E-field distribution during the training phase, enabling faster estimations [136], [137], [138], [139]. Current methods fall into two categories: supervised and self-supervised learning [23]. Supervised methods directly predict E-fields by minimising error against reference data from physics-based FEM simulations [136], [137], whereas self-supervised models predict electrical potential by optimising an energy function during training [138]. SlicerTMS, a recent extension of the open-source medical imaging platform 3D Slicer, delivers real-time E-field modelling by leveraging learning-based solvers [139].

C. Benchmarks and Metrics

The primary performance metrics for neuronavigation systems in Robo-TMS are accuracy and precision. Accuracy measures how closely the actual stimulation spot aligns with the intended brain target, typically quantified as the Euclidean distance and relative angle between the target and the actual stimulation spot, expressed in *mm* and °. Precision refers to the system's ability to consistently return to the same target across multiple attempts, also measured in *mm* and °, usually as the standard deviation of repeated localisations at the same location. Precision is essential for repetitive TMS (rTMS), where repeated targeting is required over multiple sessions. While accuracy is about hitting the target spot, precision is about consistently hitting the same spot. A system can be precise but not accurate if it consistently deviates from the target by a fixed offset. Accuracy is often influenced by registration method, imaging quality in optical tracking, and the use of individualised MRIs, while precision depends on calibration method, spatial consistency of the optical tracking system, and repeatability of the robot's movements [79].

Evaluating spatial accuracy and precision in neuronavigation systems remains challenging, particularly in living tissues where uncertainties persist. Research often focuses on optimising specific aspects of accuracy and precision under controlled conditions and uses different benchmarks (simulation, phantoms, etc) for comparison. The TABLE II lists typical benchmarks in current literature, facilitating comparative analysis of spatial accuracy and precision among methods.

Additional performance metrics relevant to neuronavigation systems in Robo-TMS include calibration and registration time [152], real-time performance of E-field modelling, effective tracking range like FOV, and user satisfaction gathered through surveys. These supplementary criteria offer a broader perspective on system performance in clinical contexts, providing a more comprehensive foundation for evaluating advancements in neuronavigation systems.

TABLE II
THE COMPARISON OF TYPICAL BENCHMARKS

Benchmarks	Methods	Advantages	Disadvantages	References
Simulations	Simulations are computer-generated models that replicate neuronavigation processes under idealised conditions. They are often used in the early stages of system development to test and predict system performance, including spatial accuracy and precision.	• Fast and cost-effective for early testing. • Can model a wide range of scenarios without requiring physical subjects or equipment. • Provides a controlled environment, allowing developers to isolate and test specific variables.	• May oversimplify real-world complexities, such as tissue deformation or sensor inaccuracies. • Does not account for human or biological variability. • Limited to theoretical validation, requiring further practical tests.	[59], [79], [140], [141]
Phantoms	Phantoms are artificial models that replicate human anatomy, typically used to physically test neuronavigation systems. These models can range from simple geometric forms to highly detailed replicas of the skull, brain, or head tissues.	• Provides a realistic, hands-on way to validate system performance. • Allows for repeated testing under consistent conditions. • Avoids ethical concerns related to human trials.	• May not fully replicate the complexities, such as heterogeneity and conductivity in live tissues. • Limited in representing the dynamic movements or changes that occur in real scenarios. • Once constructed, phantoms are fixed and do not account for inter-subject variability.	[51], [77], [142]–[146]
Landmark-based Coordinates	The landmark-based coordinate system, such as Talairach coordinates and the 10–20 system, is a standardised brain mapping framework based on anatomical landmarks.	• Can handle partial individual differences, like brain size and overall shape. • Well-established in clinical practice and easy to implement. • Non-invasive and safe.	• Template-based and may not accurately reflect individual anatomical differences. • Highly dependent on operation, introducing subjective errors. • Low resolution.	[147]
Optical Tracking	Optical tracking systems use cameras to track the pose of markers attached to the subject's head or tools in real-time. It can be employed to compare errors of various localisation methods for the same hotspot.	• Provides real-time pose feedback during navigation. • Widely used in clinical practice, making it an established method. • Non-invasive, and compatible with a range of clinical setups.	• Requires a direct line of sight between the camera and markers during procedures. • Markers may shift during procedures, introducing errors. • Difficult to locate the error of the system itself due to external factors like lighting or reflections.	[33], [53], [93], [148]–[152]
3D Scans	3D scans from MRI, CT, depth cameras and lidars, represent the head and tool within a unified observation space, enabling direct comparison of actual relative poses with ideal reference values.	• Provides highly detailed anatomical information and accurate relative poses. • Non-invasive.	• Cannot be processed in real-time. • May involve complex post-processing steps, like aligning the scan with the anatomy. • Device-dependent and can be expensive.	[80], [83]
Direct Electrical Cortical Stimulation (DECS)	DECS is a technique in which electrical impulses are applied directly to the brain during surgery to study the relationship between cortical structure and systemic function, which provides real-time feedback by observing motor or sensory responses to stimulation.	• Considered the gold standard for accuracy as it provides physiological confirmation of navigation. • Provides direct, real-time validation in live subjects.	• Invasive, requiring an open-skull procedure and limited to intraoperative settings. • Only applicable in highly specific clinical cases, primarily during neurosurgery. • Ethical and practical limitations prevent it from being a routine validation tool.	[28], [153]–[157]

V. CONTROL SYSTEMS

The goal of the Robo-TMS control system is to meet two primary clinical requirements: compensating for head movement to maintain the stimulation target in real-time, and sustaining a consistent coil-to-head contact force to ensure reliable contact while minimising the risk of discomfort or injuries.

A. Motion Compensation

In conventional TMS setups, the coil is mounted on a static holder, and subjects are instructed to avoid head movement, often with the aid of head restraints [39]. In contrast, Robo-TMS allows head movement during treatment sessions hence improving comfort. To maintain the spatial relationship between the coil and the head and achieve accurate stimulation, the robot needs to actively compensate for the subject's head movement. This spatial relationship between the TMS coil and the subject's head can be represented using a homogeneous transformation matrix:

$$\mathbf{T} = \begin{bmatrix} \mathbf{R} & \mathbf{t} \\ \mathbf{0}^\top & 1 \end{bmatrix} \in \mathbb{R}^{4\times4} \tag{2}$$

where $\mathbf{T}$ lies in the special Euclidean group $SE(3)$, $\mathbf{R}$ is a rotation matrix in the special orthogonal group $SO(3)$ and $\mathbf{t} \in \mathbb{R}^3$ is a translation vector. We denote transformations from one frame to another as ${}^{A}\mathbf{T}_{B}$, representing a transformation that converts coordinates in frame $\{B\}$ to frame $\{A\}$. Accordingly, the relationship between the TMS coil and the subject's head can be represented as ${}^{head}\mathbf{T}_{coil} = {}^{coil}\mathbf{T}_{head}{}^{-1}$.

The goal of Robo-TMS can then be expressed in terms of the clinical requirement for stimulation targeting as:

$${}^{head}\mathbf{T}^{*}_{coil} = {}^{head}\mathbf{T}_{MRI} \cdot {}^{MRI}\mathbf{T}^{*}_{coil} \tag{3}$$

where $\{head\}$ is the subject's head frame, $\{coil\}$ is the TMS coil frame, and $\{MRI\}$ is the 3D MRI frame. The transformation ${}^{head}\mathbf{T}_{MRI}$ is obtained through registration, while ${}^{MRI}\mathbf{T}^{*}_{coil}$ specifies the clinical requirement by defining the stimulation target clinicians aim to place the coil on.

In contrast to this clinical requirement in (3), the control objective is defined by an alternative expression:

$${}^{head}\mathbf{T}^{*}_{coil} = {}^{head}\mathbf{T}_{cam} \cdot {}^{cam}\mathbf{T}_{robot} \cdot {}^{robot}\mathbf{T}^{*}_{end} \cdot {}^{end}\mathbf{T}_{coil} \tag{4}$$

where $\{cam\}$ is the optical tracking camera's base frame, $\{robot\}$ is the robot's base frame, $\{end\}$ is the robot's

end-effector frame. Here, ${}^{cam}\mathbf{T}_{robot}$ and ${}^{end}\mathbf{T}_{coil}$ are determined during calibration, while ${}^{head}\mathbf{T}_{cam} = {}^{cam}\mathbf{T}_{head}{}^{-1}$ is acquired in real-time from the optical tracking system. As a result, ${}^{robot}\mathbf{T}^{*}_{end}$ represents the real-time control target, which can be calculated by solving equations (3) and (4) in the given ${}^{head}\mathbf{T}^{*}_{coil}$ [32], [98].

For cases where the optical tracking system cannot be fixed in the operating room, motion compensation can be reformulated as a tracking problem. At the cost of maintaining a line of sight to both the head and end-effector markers throughout the procedure, this method requires only the transformation ${}^{coil}T_{end}$ to be calibrated in advance [33]. The formulation is given by:

$$\begin{aligned} &{}^{cam}\mathbf{T}_{coil} \cdot {}^{coil}\mathbf{T}_{end} \cdot {}^{end}\mathbf{T}_{robot} \\ &= {}^{cam}\mathbf{T}_{head} \cdot {}^{head}\mathbf{T}^{*}_{coil} \cdot {}^{coil}\mathbf{T}_{end} \cdot {}^{end}\mathbf{T}^{*}_{robot} \end{aligned} \tag{5}$$

where ${}^{coil}\mathbf{T}_{end}$ is pre-determined via calibration, ${}^{cam}\mathbf{T}_{head}$ and ${}^{cam}\mathbf{T}_{coil}$ are obtained in real-time from optical tracking, and ${}^{end}\mathbf{T}_{robot}$ is provided by the robot arm. The control target ${}^{end}\mathbf{T}^{*}_{robot}$ is then solved using the clinical requirement ${}^{head}\mathbf{T}^{*}_{coil}$. This method eliminates the need for ${}^{cam}\mathbf{T}_{robot}$, allowing the use of a mobile camera.

B. Contact Force Control

Sustaining a consistent coil-to-head contact force is another essential clinical requirement for Robo-TMS, as it ensures reliable contact while minimising the excessive pressure which may cause discomfort or injuries to the subject. As the absence of force feedback is a known limitation [149], contact force control is strongly recommended in Robo-TMS. Integrating a force or torque sensor between the robot's end-effector and the coil allows Robo-TMS to monitor and regulate the coil's contact with the head surface, ensuring sufficient contact without discomfort or injuries. To further improve force accuracy, one study estimates the shape of the deformable coil cable to compensate for the dynamic forces applied to the robot's end-effector [29], [158].

Accurately modelling the subject's head surface is challenging due to variations in skull shape, hair volume, and underlying tissue composition. Additionally, the subject's head remains unconstrained during the TMS procedure. Sustaining a consistent coil-to-head contact force is essential to ensure reliable contact under modelling and motion uncertainties while minimising the excessive pressure which may cause discomfort and injuries. Two main force control methods adopted in Robo-TMS are impedance control [32], [43] and force/position hybrid control [146], [159]. For both control methods, current research typically adopts a two-stage control strategy: an initial free-space movement phase when the coil is relatively far from the subject's head, followed by an intra-operative phase that maintains a force normal to the subject's head surface (constrained-space movement). A study indicates that a normal force of less than 10N is typically applied to keep the coil in close contact with the head surface without causing discomfort [34]. In future developments, exploring advanced force control strategies used in other surgical robotic systems, such as model predictive control with force feedback [160] and learning-based force control [161], may enhance adaptability and robustness under anatomical variability and motion uncertainty.

C. Safety Assurance

In industrial applications, safety can be guaranteed by keeping operators outside the robot's workspace or by halting the system if a person approaches too closely. However, in Robo-TMS, subjects must remain within the robot's workspace. The need for close interaction with the human environment makes Robo-TMS design uniquely challenging, as any system failure could be critical. For safe robot-human interaction, the system must operate with high reliability and adhere to strict safety constraints.

Safety requirements for Robo-TMS can be divided into two levels: hardware and software. On the hardware level, researchers typically incorporate safety norms by adding power buttons, emergency stops, start buttons, and collision sensors. Design considerations also include limiting the robot's movement to a confined workspace through specialised structural integration [47]. On the software level, because trajectory planning and execution remain complex, errors may occur during operation to cause harmful collisions for subjects. To mitigate risks, motion limits and monitoring systems are essential, including speed limits, joint limits, contact force monitoring, movement tracking, and watchdog timers [6], [17].

VI. Discussion

Robo-TMS enhances conventional TMS by integrating advanced robotics, enabling more accurate and repeatable stimulation targeting, which streamlines the treatment process and significantly increases its efficacy. Despite significant progress, Robo-TMS remains in its early stages, with a noticeable gap between the development of robotic technologies and clinical requirements. Furthermore, these advancements introduce new concerns that require careful consideration. This section explores the clinical implications, current challenges, and future directions, focusing on how to bridge the gap between medical demands and engineering innovations.

A. Clinical Implications

In this part, we will discuss the application of Robo-TMS in a clinical context, highlighting the importance of keeping clinical scenarios in mind when integrating cutting-edge robotic technologies.

1) Reproducible Treatment: The Robo-TMS system significantly enhances clinical performance by delivering highly accurate and repeatable stimulation to specific brain regions, which is crucial for targeting small or deep brain structures [31], [151]. Unlike conventional TMS, which suffers from operator variability, robotic systems provide reproducible stimulation across sessions, improving clinical outcomes. Integrated optical tracking systems compensate for head movements, ensuring accurate stimulation throughout rTMS procedures [152]. Additionally, neuronavigation systems enable customised protocols tailored to each subject's neuroanatomy, maintaining consistent efficacy over long-term treatment courses and further enhancing therapeutic reliability and quality of care [93], [162].

2) Accurate Brain Mapping: The high targeting accuracy of Robo-TMS, typically within a few millimetres, incorporates factors such as robot arm flexibility and neuronavigation accuracy. This capability has made Robo-TMS a valuable tool for brain mapping, facilitating the study of brain structure-function relationships [10], [11], [12], [163], [164]. Clinically, brain mapping is increasingly employed for preoperative motor and language function mapping in subjects with brain tumours [28], [165]. Although language mapping tends to show lower concordance with intraoperative cortical mapping compared to motor mapping [9], TMS-guided mapping has been shown to reduce postoperative deficits with improved surgical outcomes, particularly when tumours near motor pathways [166], [167], [168].

3) Reduced Side Effects: The accuracy of Robo-TMS significantly reduces the risk of side effects by targeting specific regions without affecting unintended regions. This contrasts with non-focal electroconvulsive therapy, where non-specific stimulation frequently leads to generalised seizures [6]. In a study of 733 brain tumour subjects, including 50% with a seizure history, motor and language mapping with neuronavigation systems was found to be safe and well-tolerated [16]. Specifically, researchers used the visual analogue scale (VAS) to assess discomfort (VAS 1-3) and pain (VAS >3) and found that discomfort occurred in only 5.1% of motor mapping cases and 23.4% of language mapping cases, with minimal pain during motor mapping (0.4%) but higher pain rates during language mapping (69.5%). Despite the high seizure risk of the subjects, no seizures were observed during the procedures, and no nTMS-related seizures had been reported elsewhere [6], highlighting its safety for motor and language mapping.

4) Improved Clinician Support: In conventional TMS, clinicians manually place the coil and continuously monitor its pose throughout the session, leading to increased fatigue and stress [33]. Repeated exposure to magnetic fields and frequent physical interaction between clinicians and subjects raise concerns about long-term safety and infection transmission risks [6]. By automating coil placement and stimulation delivery, Robo-TMS can alleviate clinician fatigue and stress. By reducing direct contact, it minimises magnetic field exposure and lowers the risk of human-to-human infection transmission [169]. The integration of robotic technologies not only optimises clinical outcomes but also improves working conditions for clinicians.

5) Potential Discomfort for Subjects: While it offers significant benefits, Robo-TMS may also introduce potential discomfort for subjects [16], [31], [61]. A common concern in all rTMS treatments is the noise from the coil, which can be particularly unsettling for some individuals [4]. For instance, sound pressure levels can exceed 76dB(A) at 25cm during a 20Hz pulse train at maximum stimulator output [170]. Additionally, the presence of robots may cause fear or anxiety in individuals unfamiliar with robotic systems. Moreover, the continuous pressure exerted by the coil on the subject's head can lead to musculoskeletal discomfort [6]. The headband, which secures optical tracking markers, may further cause irritation or discomfort during prolonged sessions [82]. Although these factors are secondary to the primary clinical objectives, addressing them is crucial for enhancing subject comfort and preventing premature termination of Robo-TMS treatments.

B. Current Challenges

Despite advancements in Robo-TMS, its clinical adoption remains limited, highlighting a gap between medical needs and engineering innovations. Accessibility is identified as the foremost barrier to broader clinical adoption, driven by unverified clinical applicability, high operational complexity, and substantial implementation costs.

1) Unverified Clinical Applicability: Although Robo-TMS aims to deliver more accurate and repeatable stimulation, the clinical significance of this advantage remains unclear [171], [172]. The complex and poorly understood relationships among TMS stimulation, brain structure, neurological function, and clinical outcomes make it difficult to define how accurate the system needs to be [3], [173]. The lack of fine-scale brain atlases and comprehensive neuroscientific models further complicates target selection for effective therapy [99]. Moreover, it remains to be verified in clinical practice whether Robo-TMS offers substantial clinical benefits over conventional TMS procedures. Evidence-based guidelines are needed to clarify when and how Robo-TMS should be used. Finally, the engineering assumption of head rigidity limits applicability [78], [86], excluding subjects with involuntary facial movements and narrowing the scope of potential subjects.

2) High Operational Complexity: Excessive manual intervention in calibration and registration is a major contributor to the high operational complexity of Robo-TMS [33]. Although these steps are critical for maintaining stimulation efficacy, they are among the least automated aspects of the system. Workspace calibration must be repeated whenever the stimulation coil is changed or the operating room is rearranged. Manual registration involves identifying corresponding landmarks on the subject's head and MRI, making it time-consuming and heavily reliant on operator expertise [24], [82]. Stimulation intensity calibration must also be performed individually, as it depends on each subject's neuroanatomy. These labour-intensive procedures are prone to subjective errors, which may compromise efficacy. Moreover, reliance on markers introduces further complexity, as any displacement during treatment often necessitates re-calibration or re-registration, thereby extending the overall workflow [20].

3) Substantial Implementation Costs: High implementation costs remain a major barrier to the widespread clinical adoption of Robo-TMS. Advanced robotic platforms, optical tracking systems, and precise neuronavigation tools require substantial upfront investment and ongoing maintenance [56], [77]. Additionally, the cost of acquiring MRIs for registration and training clinicians and technicians further inflates expenses. Although cost-effective alternatives, such as personalised helmet-based coil localisation [174], have been proposed in clinical practice, they often compromise flexibility and adaptability. These challenges highlight the pressing need to reduce system complexity and operational costs to support broader deployment.

C. Future Directions

The key technical objectives of Robo-TMS are achieving greater accuracy, repeatability, and efficiency, while improving user-friendliness and lowering costs are prerequisites for large-scale adoption. To address these priorities, the following future directions can be explored.

1) Reducing Manual Intervention: While many steps in Robo-TMS have been automated, significant manual intervention remains in calibration and registration. These steps are time-consuming and heavily reliant on the operator's expertise, limiting both efficiency and accuracy [79], [175] while inflating training costs [20]. Advancements in robotics offer promising solutions to minimise manual intervention. For instance, workspace self-calibration could eliminate the assumption of fixed transformations between the camera and robot base frames, enabling the system to adapt to alignment shifts or allowing clinicians to move the camera for optimal views during procedures [33]. Similarly, self-registration methods could utilise natural facial features for automated head-to-MRI alignment, thereby reducing manual errors [84]. Incorporating non-rigid registration methods could further relax the need for subjects to replicate their expressions during MRI scanning, minimising the effort required to ensure proper alignment [78], [86].

2) Enhancing System Performance: Enhancing accuracy, repeatability, and real-time performance remains a core goal in Robo-TMS. These improvements are intrinsically linked to the capabilities of neuronavigation systems. Insights from research in both Robo-TMS and advanced robotics highlight promising developments. For instance, surface-based registration accuracy can be improved by collecting more scalp data points, paving the way for more automated solutions [79], [176]. Marker-less tracking methods, employing 3D laser scanning, TOF-based cameras, or structured-light cameras, directly track head movements without relying on conventional stereo cameras and head markers [53], [84], [177]. This method not only eliminates errors associated with markers and digitiser tools but also enhances subject comfort by removing the need for headbands, offering improved accuracy in specific scenarios [83]. Furthermore, learning-based E-field modelling significantly enhances real-time performance, further advancing the ability to deliver immediate and effective treatments [23].

3) Achieving Personalised Treatment: Stimulation intensities in TMS are typically expressed as a percentage of MT to ensure safety and standardisation across subjects and stimulation spots [87]. However, this percentage-based method can be vague and indirect, as it fails to fully account for individual neuroanatomical variations, differences in stimulation spots, and the diversity of coils and devices used [141]. Future advancements in neuroanatomy exploration and accurate E-field modelling [178] may allow for stimulation intensities to be defined in absolute units, such as current intensity mA, enabling more accurate subject-specific dosages. Moreover, automating the stimulation intensity calibration in Robo-TMS could further minimise subjective variability and achieve repeatable treatment [90].

4) Minimising Implementation Barriers: Clinicians often rely on individual MRIs for accurate registration in Robo-TMS, but their high cost and the need for specialised equipment pose barriers [4]. Additionally, it is uncommon for subjects to undergo expensive MRI scans in conventional TMS treatments. Emerging brain mapping methods offer a promising alternative by generating individualised MRIs from group or average data with sufficient accuracy [24], [148]. This innovation eliminates the need for MRI scans prior to procedures, thereby minimising implementation barriers. Moreover, while industrial robot-based Robo-TMS systems have become more accessible due to the widespread adoption of industrial robots [29], [32], [33], the expansion of the Robo-TMS market is expected to drive the re-emergence of specialised systems with enhanced clinical features [31], [47]. The broader adoption of either industrial or specialised systems is also expected to further reduce costs through economies of scale.

5) Streamlining Stimulation Workflow: In Robo-TMS, even minor movement or change in stimulation spots require physically moving the coil, which can be slow due to the robot arm's mechanical limitations and the need for accurate localisation near the scalp to ensure efficacy and safety. Advanced integration, such as robot-assisted mTMS, overcomes these challenges by using mTMS to adjust stimulation spots rapidly within small regions without moving the coil, while the robot arm can make slower adjustments when needed for larger regions [56]. Combining the capabilities of Robo-TMS with mTMS, such integration potentially improves repeatability, reduces treatment duration, and enhances subject comfort by streamlining the stimulation workflow [57].

VII. Conclusion

Robo-TMS shows great promise in enhancing the accuracy and repeatability of conventional TMS treatment; however, its clinical adoption remains limited, highlighting a gap between medical needs and engineering innovations. This review systematically analyses four critical aspects—hardware and integration, calibration and registration, neuronavigation systems, and control systems—to identify current engineering challenges linking medical requirements. Accessibility is identified as the foremost barrier of Robo-TMS, driven by unverified clinical applicability, high operational complexity, and substantial implementation costs. Emerging technologies, including marker-less tracking, non-rigid registration, learning-based E-field modelling, individualised MRI generation, Robo-mTMS, and automated calibration and registration, present promising pathways to address these challenges, hence could potentially facilitate the clinical translation and broader adoption of Robo-TMS.

References

[1] A. T. Barker, R. Jalinous, and I. L. Freeston, "Non-invasive magnetic stimulation of human motor cortex," *Lancet*, vol. 325, no. 8437, pp. 1106–1107, May 1985.

[2] S. Groppa et al., "A practical guide to diagnostic transcranial magnetic stimulation: Report of an IFCN committee," *Clin. Neurophysiol.*, vol. 123, no. 5, pp. 858–882, May 2012.

[3] H. R. Siebner et al., "Transcranial magnetic stimulation of the brain: What is stimulated?—A consensus and critical position paper," *Clin. Neurophysiol.*, vol. 140, pp. 59–97, Jan. 2022.

[4] D. J. Edwards et al., *A Practical Manual for Transcranial Magnetic Stimulation*. Cham, Switzerland: Springer, 2024.

[5] M. J. Friedrich, "Depression is the leading cause of disability around the world," *JAMA*, vol. 317, no. 15, p. 1517, Apr. 2017.

[6] S. Rossi et al., "Safety and recommendations for TMS use in healthy subjects and patient populations, with updates on training, ethical and regulatory issues: Expert guidelines," *Clin. Neurophysiol.*, vol. 132, no. 1, pp. 269–306, Jan. 2021.

[7] V. Di Lazzaro et al., "Diagnostic contribution and therapeutic perspectives of transcranial magnetic stimulation in dementia," *Clin. Neurophysiol.*, vol. 132, no. 10, pp. 2568–2607, Oct. 2021.

[8] S. Vucic et al., "Clinical diagnostic utility of transcranial magnetic stimulation in neurological disorders. Updated report of an IFCN committee," *Clin. Neurophysiol.*, vol. 150, pp. 131–175, Jun. 2023.

[9] A. F. Haddad, J. S. Young, M. S. Berger, and P. E. Tarapore, "Preoperative applications of navigated transcranial magnetic stimulation," *Frontiers Neurol.*, vol. 11, Jan. 2021, Art. no. 628903.

[10] A. Giuffre et al., "Reliability of robotic transcranial magnetic stimulation motor mapping," *J. Neurophysiol.*, vol. 125, no. 1, pp. 74–85, Jan. 2021.

[11] C. K. Kahl et al., "Active versus resting neuro-navigated robotic transcranial magnetic stimulation motor mapping," *Physiolog. Rep.*, vol. 10, no. 12, p. 15346, Jun. 2022.

[12] C. K. Kahl et al., "Reliability of active robotic neuro-navigated transcranial magnetic stimulation motor maps," *Exp. Brain Res.*, vol. 241, no. 2, pp. 355–364, Feb. 2023.

[13] J. Ruohonen and J. Karhu, "Navigated transcranial magnetic stimulation," *Neurophysiologie Clinique/Clinical Neurophysiol.*, vol. 40, no. 1, pp. 7–17, Mar. 2010.

[14] J. C. Horvath, J. M. Perez, L. Forrow, F. Fregni, and A. Pascual-Leone, "Transcranial magnetic stimulation: A historical evaluation and future prognosis of therapeutically relevant ethical concerns," *J. Med. Ethics*, vol. 37, no. 3, pp. 137–143, Mar. 2011.

[15] S. L. Cohen, M. Bikson, B. W. Badran, and M. S. George, "A visual and narrative timeline of U.S. FDA milestones for transcranial magnetic stimulation (TMS) devices," *Brain Stimulation*, vol. 15, no. 1, pp. 73–75, Jan. 2022.

[16] P. E. Tarapore et al., "Safety and tolerability of navigated TMS for preoperative mapping in neurosurgical patients," *Clin. Neurophysiol.*, vol. 127, no. 3, pp. 1895–1900, Mar. 2016.

[17] S. R. Kantelhardt et al., "Robot-assisted image-guided transcranial magnetic stimulation for somatotopic mapping of the motor cortex: A clinical pilot study," *Acta Neurochirurgica*, vol. 152, no. 2, pp. 333–343, Feb. 2010.

[18] T. Wagner, A. Valero-Cabré, and Á. Pascual-Leone, "Noninvasive human brain stimulation," *Annu. Rev. Biomed. Eng.*, vol. 9, no. 1, pp. 527–565, 2007.

[19] K. Cleary and T. M. Peters, "Image-guided interventions: Technology review and clinical applications," *Annu. Rev. Biomed. Eng.*, vol. 12, no. 1, pp. 119–142, Jul. 2010.

[20] J. A. Smith, J. Jivraj, R. Wong, and V. Yang, "30 years of neurosurgical robots: Review and trends for manipulators and associated navigational systems," *Ann. Biomed. Eng.*, vol. 44, no. 4, pp. 836–846, Apr. 2016.

[21] G. Pivazyan, F. A. Sandhu, A. R. Beaufort, and B. W. Cunningham, "Basis for error in stereotactic and computer-assisted surgery in neurosurgical applications: Literature review," *Neurosurgical Rev.*, vol. 46, no. 1, Dec. 2022, Art. no. 20.

[22] J. A. Pérez-Benítez, P. Martínez-Ortiz, and J. Aguila-Muñoz, "A review of formulations, boundary value problems and solutions for numerical computation of transcranial magnetic stimulation fields," *Brain Sci.*, vol. 13, no. 8, p. 1142, Jul. 2023.

[23] T. Y. Park, L. Franke, S. Pieper, D. Haehn, and L. Ning, "A review of algorithms and software for real-time electric field modeling techniques for transcranial magnetic stimulation," *Biomed. Eng. Lett.*, vol. 14, no. 3, pp. 393–405, May 2024.

[24] C. Gao et al., "Individualized brain mapping for navigated neuromodulation," *Chin. Med. J.*, vol. 137, no. 5, pp. 508–523, 2024.

[25] U. Herwig et al., "Transcranial magnetic stimulation in therapy studies: Examination of the reliability of 'standard" coil positioning by neuronavigation," *Biol. Psychiatry*, vol. 50, no. 1, pp. 58–61, 2001.

[26] R. Sparing, D. Buelte, I. G. Meister, T. Pauš, and G. R. Fink, "Transcranial magnetic stimulation and the challenge of coil placement: A comparison of conventional and stereotaxic neuronavigational strategies," *Hum. Brain Mapping*, vol. 29, no. 1, pp. 82–96, Jan. 2008.

[27] X. Fang, M. Liu, C. Lu, Y. Zhao, and X. Liu, "Current status and potential application of navigated transcranial magnetic stimulation in neurosurgery: A literature review," *Chin. Neurosurgical J.*, vol. 5, no. 1, p. 12, Dec. 2019.

[28] H.-R. Jeltema et al., "Comparing navigated transcranial magnetic stimulation mapping and 'gold standard' direct cortical stimulation mapping in neurosurgery: A systematic review," *Neurosurgical Rev.*, vol. 44, no. 4, pp. 1903–1920, 2021.

[29] L. Richter, *Robotized Transcranial Magnetic Stimulation*. New York, NY, USA: Springer New York, 2013.

[30] L. Matthäus, "A robotic assistance system for transcranial magnetic stimulation and its application to motor cortex mapping, "A robotic assistance system for transcranial magnetic stimulation and its application to motor cortex mapping," Ph.D. dissertation, Inst. Robot. Cogn. Syst., Univ. Lübeck, Lübeck, Germany, 2008.

[31] R. Ginhoux et al., "A custom robot for transcranial magnetic stimulation: First assessment on healthy subjects," in *Proc. 35th Annu. Int. Conf. IEEE Eng. Med. Biol. Soc. (EMBC)*, Jul. 2013, pp. 5352–5355.

[32] A. Noccaro, A. Mioli, M. D'Alonzo, M. Pinardi, G. D. Pino, and D. Formica, "Development and validation of a novel calibration methodology and control approach for robot-aided transcranial magnetic stimulation (TMS)," *IEEE Trans. Biomed. Eng.*, vol. 68, no. 5, pp. 1589–1600, May 2021.

[33] I. Xygonakis et al., "Transcranial magnetic stimulation robotic assistant: Towards a fully automated stimulation session," in *Proc. 10th IEEE RAS/EMBS Int. Conf. Biomed. Robot. Biomechatronics (BioRob)*, Berlin, Germany, Sep. 2024, pp. 1401–1408.

[34] W. Zakaria and W. Nurshazwani, "Force-controlled transcranial magnetic stimulation (TMS) robotic system," M.S. thesis, School Mech. Syst. Eng., Newcastle University, Newcastle upon Tyne, U.K., 2012.

[35] C. Lebossé, "Robotic image-guided transcranial magnetic stimulation," *Int. J. Comput. Assist. Radiol. Surgery*, vol. 1, p. 137, Jun. 2006.

[36] *Magstim Horizon Lite*. (2025). Accessed: Apr. 7, 2025. [Online]. Available: https://www.magstim.com/product/horizon-lite/

[37] *Axilum Robotics TMS-Cobot*. (2025). *Axilumrobotics Robotics*. Accessed: Apr. 7, 2025. [Online]. Available: https://www.axilumrobotics.com/en/tms-cobot-features/

[38] *Yiruide Mag-Aim*. (2025). Accessed: Apr. 7, 2025. [Online]. Available: https://www.yiruide.com/news/114.html

[39] E. P. Chronicle, A. J. Pearson, and C. Matthews, "Development and positioning reliability of a TMS coil holder for headache research," *Headache, J. Head Face Pain*, vol. 45, no. 1, pp. 37–41, Jan. 2005.

[40] S. Narayana et al., "Use of neurosurgical robot for aiming and holding in cortical TMS experiments," *NeuroImage*, vol. 11, no. 5, p. S471, May 2000.

[41] J. L. Lancaster, S. Narayana, D. Wenzel, J. Luckemeyer, J. Roby, and P. Fox, "Evaluation of an image-guided, robotically positioned transcranial magnetic stimulation system," *Human Brain Mapping*, vol. 22, no. 4, pp. 329–340, Aug. 2004.

[42] L. Matthäus, "Robotized TMS for motion compensated navigated brain stimulation," *Int. J. Comput. Assist. Radiol. Surgery*, vol. 1, no. S1, pp. 137–145, 2006.

[43] G. Pennimpede et al., "Hot spot hound: A novel robot-assisted platform for enhancing TMS performance," in *Proc. 35th Annu. Int. Conf. IEEE Eng. Med. Biol. Soc. (EMBC)*, Jul. 2013, pp. 6301–6304.

[44] G. D. Todd, A. Abdellatif, and A. Sabouni, "BRAIN initiative: Transcranial magnetic stimulation automation and calibration," in *Proc. 36th Annu. Int. Conf. IEEE Eng. Med. Biol. Soc.*, Chicago, IL, USA, Aug. 2014, pp. 502–505.

[45] J. J. de Jong, A. H. A. Stienen, V. van der Wijk, M. Wessels, and H. van der Kooij, "A method for evaluation and comparison of parallel robots for safe human interaction, applied to robotic TMS," in *Proc. 4th IEEE RAS EMBS Int. Conf. Biomed. Robot. Biomechatronics (BioRob)*, Jun. 2012, pp. 986–991.

[46] C. Lebosse, P. Renaud, B. Bayle, M. de Mathelin, O. Piccin, and J. Foucher, "A robotic system for automated image-guided transcranial magnetic stimulation," in *Proc. IEEE/NIH Life Sci. Syst. Appl. Workshop*, Bethesda, MD, USA, Nov. 2007, pp. 55–58.

[47] L. Zorn et al., "Design and evaluation of a robotic system for transcranial magnetic stimulation," *IEEE Trans. Biomed. Eng.*, vol. 59, no. 3, pp. 805–815, Mar. 2012.

[48] X. Yi and R. Bicker, "Design of a robotic transcranial magnetic stimulation system," in *Proc. IEEE Conf. Robot., Autom. Mechatronics*, Singapore, Jun. 2010, pp. 78–83.

[49] A. Zangen, Y. Roth, B. Voller, and M. Hallett, "Transcranial magnetic stimulation of deep brain regions: Evidence for efficacy of the H-coil," *Clin. Neurophysiol.*, vol. 116, no. 4, pp. 775–779, Apr. 2005.

[50] Y. Liu, S. Liu, S. Sefati, J. Tian, A. Kheradmand, and M. Armand, "Inside-out tracking and projection mapping for robot-assisted transcranial magnetic stimulation," *Proc. SPIE*, vol. 11931, pp. 57–70, Feb. 2022.

[51] P. M. Kebria, S. Nahavandi, P. Enticott, and F. Bello, "Haptically-enabled robotic teleoperation for transcranial magnetic stimulation (TeleTMS)," in *Proc. IEEE Int. Conf. Syst., Man, Cybern. (SMC)*, Oct. 2023, pp. 2100–2105.

[52] Z. Xiao, Q. Ruan, and X. Wang, "CortexBot: 3D visual fusion of robotic neuronavigated TMS system," in *Proc. IEEE Int. Conf. Cyborg Bionic Syst. (CBS)*, Oct. 2018, pp. 406–411.

[53] Y. Chen, W. Xin, L. ZongJie, and S. HuanRan, "No-attachment head tracking method of robotic transcranial magnetic stimulation based on vision sensor," in *Proc. 16th Int. Conf. Control, Autom., Robot. Vis. (ICARCV)*. Shenzhen, China: IEEE, Dec. 2020, pp. 1366–1371.

[54] L. M. Koponen, J. O. Nieminen, and R. J. Ilmoniemi, "Multi-locus transcranial magnetic stimulation—Theory and implementation," *Brain Stimulation*, vol. 11, no. 4, pp. 849–855, Jul. 2018.

[55] J. O. Nieminen et al., "Multi-locus transcranial magnetic stimulation system for electronically targeted brain stimulation," *Brain Stimulation*, vol. 15, no. 1, pp. 116–124, Jan. 2022.

[56] R. H. Matsuda et al., "Robotic–electronic platform for autonomous and accurate transcranial magnetic stimulation targeting," *Brain Stimulation*, vol. 17, no. 2, pp. 469–472, Mar. 2024.

[57] H. Sinisalo et al., "Modulating brain networks in space and time: Multi-locus transcranial magnetic stimulation," *Clin. Neurophysiol.*, vol. 158, pp. 218–224, Feb. 2024.

[58] N. Zhang et al., "Theoretical analysis and design of an innovative coil structure for transcranial magnetic stimulation," *Appl. Sci.*, vol. 11, no. 4, p. 1960, Feb. 2021.

[59] Z.-D. Deng, S. H. Lisanby, and A. V. Peterchev, "Electric field depth–focality tradeoff in transcranial magnetic stimulation: Simulation comparison of 50 coil designs," *Brain Stimulation*, vol. 6, no. 1, pp. 1–13, Jan. 2013.

[60] S. Ueno, T. Tashiro, and K. Harada, "Localized stimulation of neural tissues in the brain by means of a paired configuration of time-varying magnetic fields," *J. Appl. Phys.*, vol. 64, no. 10, pp. 5862–5864, Nov. 1988.

[61] A. V. Peterchev et al., "Advances in transcranial magnetic stimulation technology," in *Brain Stimulation*, 1st ed., I. M. Ret, Ed., Hoboken, NJ, USA: Wiley, 2015, pp. 165–189.

[62] H. Bagherzadeh and F. Choa, "Effect of coil size on transcranial magnetic stimulation (TMS) focality," *Proc. SPIE*, vol. 11020, pp. 224–229, May 2019.

[63] M. Lu and S. Ueno, "Comparison of the induced fields using different coil configurations during deep transcranial magnetic stimulation," *PLoS ONE*, vol. 12, no. 6, Jun. 2017, Art. no. e0178422.

[64] T. Fadini et al., "H-coil: Induced electric field properties and input/output curves on healthy volunteers, comparison with a standard figure-of-eight coil," *Clin. Neurophysiol.*, vol. 120, no. 6, pp. 1174–1182, Jun. 2009.

[65] J. A. V. Membrilla, M. F. Pantoja, A. P. V. Puerta, V. H. Souza, and C. C. Sánchez, "Design of transcranial magnetic stimulation coils with optimized stimulation depth," *IEEE Access*, vol. 12, pp. 1330–1340, 2024.

[66] I. J. Rissanen, V. H. Souza, J. O. Nieminen, L. M. Koponen, and R. J. Ilmoniemi, "Advanced pipeline for designing multi-locus TMS coils with current density constraints," *IEEE Trans. Biomed. Eng.*, vol. 70, no. 7, pp. 2025–2034, Jul. 2023.

[67] A. Thielscher and T. Kammer, "Electric field properties of two commercial figure-8 coils in TMS: Calculation of focality and efficiency," *Clin. Neurophysiol.*, vol. 115, no. 7, pp. 1697–1708, Jul. 2004.

[68] M. Drakaki, C. Mathiesen, H. R. Siebner, K. Madsen, and A. Thielscher, "Database of 25 validated coil models for electric field simulations for TMS," *Brain Stimulation*, vol. 15, no. 3, pp. 697–706, May 2022.

[69] L. J. Gomez, S. M. Goetz, and A. V. Peterchev, "Design of transcranial magnetic stimulation coils with optimal trade-off between depth, focality, and energy," *J. Neural Eng.*, vol. 15, no. 4, Aug. 2018, Art. no. 046033.

[70] S. Nurmi, J. Karttunen, V. H. Souza, R. J. Ilmoniemi, and J. O. Nieminen, "Trade-off between stimulation focality and the number of coils in multi-locus transcranial magnetic stimulation," *J. Neural Eng.*, vol. 18, no. 6, Dec. 2021, Art. no. 066003.

[71] L. Richter, F. Ernst, A. Schlaefer, and A. Schweikard, "Robust real-time robot–world calibration for robotized transcranial magnetic stimulation," *Int. J. Med. Robot. Comput. Assist. Surg.*, vol. 7, no. 4, pp. 414–422, 2011.

[72] H. Wang, J. Jin, X. Wang, Y. Li, Z. Liu, and T. Yin, "Non-orthogonal one-step calibration method for robotized transcranial magnetic stimulation," *Biomed. Eng. OnLine*, vol. 17, no. 1, p. 137, Dec. 2018.

[73] J. Ha, D. Kang, and F. C. Park, "A stochastic global optimization algorithm for the two-frame sensor calibration problem," *IEEE Trans. Ind. Electron.*, vol. 63, no. 4, pp. 2434–2446, Apr. 2016.

[74] F. Ernst et al., "Non-orthogonal tool/flange and robot/world calibration," *Int. J. Med. Robot. Comput. Assist. Surgery*, vol. 8, no. 4, pp. 407–420, Dec. 2012.

[75] F. Dornaika and R. Horaud, "Simultaneous robot-world and hand-eye calibration," *IEEE Trans. Robot. Autom.*, vol. 14, no. 4, pp. 617–622, Aug. 1998.

[76] Y. Liu, J. Zhang, Z. She, A. Kheradmand, and M. Armand, "GBEC: Geometry-based hand-eye calibration," in *Proc. IEEE Int. Conf. Robot. Autom. (ICRA)*, May 2024, pp. 16698–16705.

[77] Y. Liu et al., "An image-guided robotic system for transcranial magnetic stimulation: System development and experimental evaluation," *IEEE Robot. Autom. Lett.*, vol. 10, no. 2, pp. 1936–1943, Feb. 2025.

[78] D. A. Orringer, A. Golby, and F. Jolesz, "Neuronavigation in the surgical management of brain tumors: Current and future trends," *Expert Rev. Med. Devices*, vol. 9, no. 5, pp. 491–500, Sep. 2012.

[79] A. E. Nieminen et al., "Accuracy and precision of navigated transcranial magnetic stimulation," *J. Neural Eng.*, vol. 19, no. 6, Dec. 2022, Art. no. 066037.

[80] N. Matilainen, J. Kataja, and I. Laakso, "Verification of neuronavigated TMS accuracy using structured-light 3D scans," *Phys. Med. Biol.*, vol. 69, no. 8, Apr. 2024, Art. no. 085004.

[81] R. R. Shamir, L. Joskowicz, S. Spektor, and Y. Shoshan, "Localization and registration accuracy in image guided neurosurgery: A clinical study," *Int. J. Comput. Assist. Radiol. Surg.*, vol. 4, no. 1, pp. 45–52, Jan. 2009.

[82] A. I. Omara, M. Wang, Y. Fan, and Z. Song, "Anatomical landmarks for point-matching registration in image-guided neurosurgery: Anatomical landmarks for point matching registration in IGN," *Int. J. Med. Robot. Comput. Assist. Surg.*, vol. 10, no. 1, pp. 55–64, Mar. 2014.

[83] N. Hironaga, T. Kimura, T. Mitsudo, A. Gunji, and M. Iwata, "Proposal for an accurate TMS-MRI co-registration process via 3D laser scanning," *Neurosci. Res.*, vol. 144, pp. 30–39, Jul. 2019.

[84] G. Liu et al., "Transcranial magnetic stimulation (TMS) localization by co-registration of facial point clouds," *Brain Stimulation*, vol. 16, no. 1, pp. 79–81, Jan. 2023.

[85] S. Monji-Azad, J. Hesser, and N. Löw, "A review of non-rigid transformations and learning-based 3D point cloud registration methods," *ISPRS J. Photogramm. Remote Sens.*, vol. 196, pp. 58–72, Feb. 2023.

[86] P. Risholm, A. J. Golby, and W. Wells, "Multimodal image registration for preoperative planning and image-guided neurosurgical procedures," *Neurosurgery Clinics North Amer.*, vol. 22, no. 2, pp. 197–206, Apr. 2011.

[87] T. Herbsman et al., "Motor threshold in transcranial magnetic stimulation: The impact of white matter fiber orientation and skull-to-cortex distance," *Hum. Brain Mapping*, vol. 30, no. 7, pp. 2044–2055, Jul. 2009.

[88] F. Awiszus, "TMS and threshold hunting," in *Supplements to Clinical Neurophysiology*, vol. 56. Amsterdam, The Netherlands: Elsevier, 2003, pp. 13–23.

[89] J. Meincke, M. Hewitt, G. Batsikadze, and D. Liebetanz, "Automated TMS hotspot-hunting using a closed loop threshold-based algorithm," *NeuroImage*, vol. 124, pp. 509–517, Jan. 2016.

[90] S. Harquel et al., "Automatized set-up procedure for transcranial magnetic stimulation protocols," *NeuroImage*, vol. 153, pp. 307–318, Jun. 2017.

[91] A. E. Tervo, J. Metsomaa, J. O. Nieminen, J. Sarvas, and R. J. Ilmoniemi, "Automated search of stimulation targets with closed-loop transcranial magnetic stimulation," *NeuroImage*, vol. 220, Oct. 2020, Art. no. 117082.

[92] A. E. Tervo et al., "Closed-loop optimization of transcranial magnetic stimulation with electroencephalography feedback," *Brain Stimulation*, vol. 15, no. 2, pp. 523–531, Mar. 2022.

[93] A. A. de Goede, E. M. ter Braack, and M. J. A. M. van Putten, "Accurate coil positioning is important for single and paired pulse TMS on the subject level," *Brain Topography*, vol. 31, no. 6, pp. 917–930, Nov. 2018.

[94] N. D. Glossop, "Advantages of optical compared with electromagnetic tracking," *J. Bone Joint Surgery*, vol. 91, no. 1, pp. 23–28, 2009.

[95] M. Krogius, A. Haggenmiller, and E. Olson, "Flexible layouts for fiducial tags," in *Proc. IEEE/RSJ Int. Conf. Intell. Robots Syst. (IROS)*, Macau, China, Nov. 2019, pp. 1898–1903.

[96] S. Garrido-Jurado, R. Mu noz-Salinas, F. J. Madrid-Cuevas, and M. J. Marín-Jiménez, "Automatic generation and detection of highly reliable fiducial markers under occlusion," *Pattern Recognit.*, vol. 47, no. 6, pp. 2280–2292, Jun. 2014.

[97] V. H. Souza et al., "Development and characterization of the InVesalius navigator software for navigated transcranial magnetic stimulation," *J. Neurosci. Methods*, vol. 309, pp. 109–120, Nov. 2018.

[98] Z. Lin, X. Wang, and J. Yang, "Trajectory tracking control of robotic transcranial magnetic stimulation," *Int. J. Intell. Comput. Cybern.*, vol. 12, no. 2, pp. 245–259, Jun. 2019.

[99] Z.-D. Deng et al., "Device-based modulation of neurocircuits as a therapeutic for psychiatric disorders," *Annu. Rev. Pharmacol. Toxicology*, vol. 60, no. 1, pp. 591–614, Jan. 2020.

[100] K. P. Esselle and M. A. Stuchly, "Neural stimulation with magnetic fields: Analysis of induced electric fields," *IEEE Trans. Biomed. Eng.*, vol. 39, no. 7, pp. 693–700, Jul. 1992.

[101] L. Heller and D. B. Van Hulsteyn, "Brain stimulation using electromagnetic sources: Theoretical aspects," *Biophysical J.*, vol. 63, no. 1, pp. 129–138, Jul. 1992.

[102] T. A. Wagner, M. Zahn, A. J. Grodzinsky, and A. Pascual-Leone, "Three-dimensional head model simulation of transcranial magnetic stimulation," *IEEE Trans. Biomed. Eng.*, vol. 51, no. 9, pp. 1586–1598, Sep. 2004.

[103] A. Nummenmaa, M. Stenroos, R. J. Ilmoniemi, Y. C. Okada, M. S. Hämäläinen, and T. Raij, "Comparison of spherical and realistically shaped boundary element head models for transcranial magnetic stimulation navigation," *Clin. Neurophysiol.*, vol. 124, no. 10, pp. 1995–2007, Oct. 2013.

[104] X. Wei, D. Shi, M. Lu, G. Yi, and J. Wang, "Deep transcranial magnetic stimulation: Improved coil design and assessment of the induced fields using realistic head model," in *Proc. Chin. Control Conf. (CCC)*. Guangzhou, China: IEEE, Jul. 2019, pp. 3727–3731.

[105] I. Laakso, S. Tanaka, S. Koyama, V. De Santis, and A. Hirata, "Inter-subject variability in electric fields of motor cortical tDCS," *Brain Stimulation*, vol. 8, no. 5, pp. 906–913, Sep. 2015.

[106] I. Laakso, T. Murakami, A. Hirata, and Y. Ugawa, "Where and what TMS activates: Experiments and modeling," *Brain Stimulation*, vol. 11, no. 1, pp. 166–174, Jan. 2018.

[107] A. Thielscher, A. Antunes, and G. B. Saturnino, "Field modeling for transcranial magnetic stimulation: A useful tool to understand the physiological effects of TMS?" in *Proc. 37th Annu. Int. Conf. IEEE Eng. Med. Biol. Soc. (EMBC)*, Aug. 2015, pp. 222–225.

[108] J. D. Nielsen et al., "Automatic skull segmentation from MR images for realistic volume conductor models of the head: Assessment of the state-of-the-art," *NeuroImage*, vol. 174, pp. 587–598, Jul. 2018.

[109] Y. Huang, A. Datta, M. Bikson, and L. C. Parra, "Realistic volumetric-approach to simulate transcranial electric stimulation—ROAST—A fully automated open-source pipeline," *J. Neural Eng.*, vol. 16, no. 5, Oct. 2019, Art. no. 056006.

[110] A. Thielscher, A. Opitz, and M. Windhoff, "Impact of the gyral geometry on the electric field induced by transcranial magnetic stimulation," *NeuroImage*, vol. 54, no. 1, pp. 234–243, Jan. 2011.

[111] G. B. Saturnino, O. Puonti, J. D. Nielsen, D. Antonenko, K. H. Madsen, and A. Thielscher, "SimNIBS 2.1: A comprehensive pipeline for individualized electric field modelling for transcranial brain stimulation," *Brain Hum. Body Model., Comput. Hum. Model. EMBC*, vol. 2019, pp. 3–25, Jan. 2019.

[112] O. Puonti, K. Van Leemput, G. B. Saturnino, H. R. Siebner, K. H. Madsen, and A. Thielscher, "Accurate and robust whole-head segmentation from magnetic resonance images for individualized head modeling," *NeuroImage*, vol. 219, Oct. 2020, Art. no. 117044.

[113] L. J. Gomez, M. Dannhauer, L. M. Koponen, and A. V. Peterchev, "Conditions for numerically accurate TMS electric field simulation," *Brain Stimulation*, vol. 13, no. 1, pp. 157–166, Jan. 2020.

[114] U. Herwig et al., "The navigation of transcranial magnetic stimulation," *Psychiatry Res., Neuroimaging*, vol. 108, no. 2, pp. 123–131, 2001.

[115] N. Sollmann et al., "Comparison between electric-field-navigated and line-navigated TMS for cortical motor mapping in patients with brain tumors," *Acta Neurochirurgica*, vol. 158, no. 12, pp. 2277–2289, Dec. 2016.

[116] A. Bungert, A. Antunes, S. Espenhahn, and A. Thielscher, "Where does TMS stimulate the motor cortex? Combining electrophysiological measurements and realistic field estimates to reveal the affected cortex position," *Cerebral Cortex*, vol. 27, no. 11, pp. 5083–5094, Nov. 2017.

[117] D. Wang, N. I. Hasan, M. Dannhauer, A. C. Yucel, and L. J. Gomez, "Fast computational E-field dosimetry for transcranial magnetic stimulation using adaptive cross approximation and auxiliary dipole method (ACA-ADM)," *NeuroImage*, vol. 267, Feb. 2023, Art. no. 119850.

[118] N. I. Hasan, M. Dannhauer, D. Wang, Z.-D. Deng, and L. J. Gomez, "Real-time computation of brain E-field for enhanced transcranial magnetic stimulation neuronavigation and optimization," *Imag. Neurosci.*, vol. 3, Jan. 2025, doi: 10.1162/imag_a_00412.

[119] N. I. Hasan, D. Wang, and L. J. Gomez, "Fast and accurate computational E-field dosimetry for group-level transcranial magnetic stimulation targeting," *Comput. Biol. Med.*, vol. 167, Dec. 2023, Art. no. 107614.

[120] S. N. Makarov, G. M. Noetscher, T. Raij, and A. Nummenmaa, "A quasi-static boundary element approach with fast multipole acceleration for high-resolution bioelectromagnetic models," *IEEE Trans. Biomed. Eng.*, vol. 65, no. 12, pp. 2675–2683, Dec. 2018.

[121] A. T. Htet, G. B. Saturnino, E. H. Burnham, G. M. Noetscher, A. Nummenmaa, and S. N. Makarov, "Comparative performance of the finite element method and the boundary element fast multipole method for problems mimicking transcranial magnetic stimulation (TMS)," *J. Neural Eng.*, vol. 16, no. 2, Apr. 2019, Art. no. 024001.

[122] M. Stenroos and L. M. Koponen, "Real-time computation of the TMS-induced electric field in a realistic head model," *NeuroImage*, vol. 203, Dec. 2019, Art. no. 116159.

[123] M. Daneshzand et al., "Rapid computation of TMS-induced E-fields using a dipole-based magnetic stimulation profile approach," *NeuroImage*, vol. 237, Aug. 2021, Art. no. 118097.

[124] S. N. Makaroff et al., "A fast direct solver for surface-based whole-head modeling of transcranial magnetic stimulation," *Sci. Rep.*, vol. 13, no. 1, p. 18657, Oct. 2023.

[125] N. Toschi, T. Welt, M. Guerrisi, and M. E. Keck, "A reconstruction of the conductive phenomena elicited by transcranial magnetic stimulation in heterogeneous brain tissue," *Phys. Medica*, vol. 24, no. 2, pp. 80–86, Jun. 2008.

[126] I. Laakso and A. Hirata, "Fast multigrid-based computation of the induced electric field for transcranial magnetic stimulation," *Phys. Med. Biol.*, vol. 57, no. 23, pp. 7753–7765, 2012.

[127] A. Paffi et al., "A computational model for real-time calculation of electric field due to transcranial magnetic stimulation in clinics," *Int. J. Antennas Propag.*, vol. 2015, pp. 1–11, Jan. 2015.

[128] S. Silva, P. J. Basser, and P. C. Miranda, "Elucidating the mechanisms and loci of neuronal excitation by transcranial magnetic stimulation using a finite element model of a cortical sulcus," *Clin. Neurophysiol.*, vol. 119, no. 10, pp. 2405–2413, Oct. 2008.

[129] S. N. Makarov et al., "Preliminary upper estimate of peak currents in transcranial magnetic stimulation at distant locations from a TMS coil," *IEEE Trans. Biomed. Eng.*, vol. 63, no. 9, pp. 1944–1955, Sep. 2016.

[130] O. F. Afuwape, P. Rastogi, and D. Jiles, "Effect of coil positioning and orientation of the quadruple butterfly coil during transcranial magnetic stimulation," *AIP Adv.*, vol. 11, no. 1, Jan. 2021, Art. no. 015212.

[131] P. Rastogi, E. G. Lee, R. L. Hadimani, and D. C. Jiles, "Transcranial magnetic stimulation-coil design with improved focality," *AIP Adv.*, vol. 7, no. 5, May 2017, Art. no. 056705.

[132] O. Puonti, G. B. Saturnino, K. H. Madsen, and A. Thielscher, "Value and limitations of intracranial recordings for validating electric field modeling for transcranial brain stimulation," *NeuroImage*, vol. 208, Mar. 2020, Art. no. 116431.

[133] L. J. Gomez, M. Dannhauer, and A. V. Peterchev, "Fast computational optimization of TMS coil placement for individualized electric field targeting," *NeuroImage*, vol. 228, Mar. 2021, Art. no. 117696.

[134] Y. Huang, A. Datta, M. Bikson, and L. C. Parra, "ROAST: An open-source, fully-automated, realistic volumetric-approach-based simulator for TES," in *Proc. 40th Annu. Int. Conf. IEEE Eng. Med. Biol. Soc. (EMBC)*, Jul. 2018, pp. 3072–3075.

[135] S. F. W. Neggers et al., "A stereotactic method for image-guided transcranial magnetic stimulation validated with fMRI and motor-evoked potentials," *NeuroImage*, vol. 21, no. 4, pp. 1805–1817, Apr. 2004.

[136] T. Yokota et al., "Real-time estimation of electric fields induced by transcranial magnetic stimulation with deep neural networks," *Brain Stimulation*, vol. 12, no. 6, pp. 1500–1507, Nov. 2019.

[137] G. Xu, Y. Rathi, J. A. Camprodon, H. Cao, and L. Ning, "Rapid whole-brain electric field mapping in transcranial magnetic stimulation using deep learning," *PLoS ONE*, vol. 16, no. 7, Jul. 2021, Art. no. e0254588.

[138] H. Li, Z.-D. Deng, D. Oathes, and Y. Fan, "Computation of transcranial magnetic stimulation electric fields using self-supervised deep learning," *NeuroImage*, vol. 264, Dec. 2022, Art. no. 119705.

[139] L. Franke et al., "SlicerTMS: Real-time visualization of transcranial magnetic stimulation for mental health treatment," in *Proc. Int. Conf. Med. Image Comput. Comput.-Assist. Intervent*, 2024, pp. 575–585.
[140] M. Mikkonen and I. Laakso, "Effects of posture on electric fields of non-invasive brain stimulation," *Phys. Med. Biol.*, vol. 64, no. 6, Mar. 2019, Art. no. 065019.
[141] K. A. Caulfield et al., "Mitigating the risk of overdosing TMS due to coil-to-scalp distance: An electric field modeling study," *Brain Stimulation*, vol. 17, no. 4, pp. 970–974, Jul. 2024.
[142] L. Richter, R. Bruder, and A. Schweikard, "Hand-assisted positioning and contact pressure control for motion compensated robotized transcranial magnetic stimulation," *Int. J. Comput. Assist. Radiol. Surgery*, vol. 7, no. 6, pp. 845–852, Nov. 2012.
[143] L. Richter, P. Trillenberg, A. Schweikard, and A. Schlaefer, "Stimulus intensity for hand held and robotic transcranial magnetic stimulation," *Brain Stimulation*, vol. 6, no. 3, pp. 315–321, May 2013.
[144] A. Noccaro, L. Raiano, G. Di Pino, and D. Formica, "Evaluation of hand-eye and robot-world calibration algorithms for TMS application," in *Proc. 7th IEEE Int. Conf. Biomed. Robot. Biomechatronics (Biorob)*, Aug. 2018, pp. 1115–1119.
[145] G. B. Saturnino, K. H. Madsen, and A. Thielscher, "Electric field simulations for transcranial brain stimulation using FEM: An efficient implementation and error analysis," *J. Neural Eng.*, vol. 16, no. 6, Nov. 2019, Art. no. 066032.
[146] P. Jaroonsorn, P. Neranon, P. Smithmaitrie, and C. Dechwayukul, "Robot-assisted transcranial magnetic stimulation using hybrid position/force control," *Adv. Robot.*, vol. 34, no. 24, pp. 1559–1570, Dec. 2020.
[147] I. M. Young et al., "Comparison of consistency between image guided and craniometric transcranial magnetic stimulation coil placement," *Brain Stimulation*, vol. 15, no. 6, pp. 1465–1466, Nov. 2022.
[148] F. Carducci and R. Brusco, "Accuracy of an individualized MR-based head model for navigated brain stimulation," *Psychiatry Res., Neuroimaging*, vol. 203, no. 1, pp. 105–108, Jul. 2012.
[149] S. M. Goetz et al., "Accuracy of robotic coil positioning during transcranial magnetic stimulation," *J. Neural Eng.*, vol. 16, no. 5, Sep. 2019, Art. no. 054003.
[150] K. A. Caulfield, H. H. Fleischmann, C. E. Cox, J. P. Wolf, M. S. George, and L. M. McTeague, "Neuronavigation maximizes accuracy and precision in TMS positioning: Evidence from 11,230 distance, angle, and electric field modeling measurements," *Brain Stimulation*, vol. 15, no. 5, pp. 1192–1205, Sep. 2022.
[151] L. C. Dormegny-Jeanjean et al., "3D-mapping of TMS effects with automatic robotic placement improved reliability and the risk of spurious correlation," *J. Neurosci. Methods*, vol. 381, Nov. 2022, Art. no. 109689.
[152] Y. A. Chung, H. Jeong, and I. U. Song, "Robotic transcranial magnetic stimulation in the treatment of depression: A pilot study," *Brain Stimulation*, vol. 18, no. 1, p. 525, Jan. 2025.
[153] P. E. Tarapore et al., "Preoperative multimodal motor mapping: A comparison of magnetoencephalography imaging, navigated transcranial magnetic stimulation, and direct cortical stimulation: Clinical article," *J. Neurosurgery*, vol. 117, no. 2, pp. 354–362, Aug. 2012.
[154] S. M. Krieg et al., "Utility of presurgical navigated transcranial magnetic brain stimulation for the resection of tumors in eloquent motor areas: Clinical article," *J. Neurosurgery*, vol. 116, no. 5, pp. 994–1001, May 2012.
[155] S. Takahashi, P. Vajkoczy, and T. Picht, "Navigated transcranial magnetic stimulation for mapping the motor cortex in patients with rolandic brain tumors," *Neurosurgical Focus*, vol. 34, no. 4, p. E3, Apr. 2013.
[156] R. S. Indharty et al., "Comparison of direct cortical stimulation and transcranial magnetic stimulation in brain tumor surgery: Systematic review and meta analyses," *J. Neuro-Oncol.*, vol. 163, no. 3, pp. 505–514, Jul. 2023.
[157] G. Muscas et al., "Heads-up micronavigation reliability of preoperative transcranial magnetic stimulation maps for the motor function: Comparison with direct cortical stimulation," *Operative Neurosurgery*, vol. 26, no. 2, pp. 173–179, Feb. 2024.
[158] J. Zhang, Z. Zhang, Y. Liu, Y. Chen, A. Kheradmand, and M. Armand, "Realtime robust shape estimation of deformable linear object," in *Proc. IEEE Int. Conf. Robot. Autom. (ICRA)*, May 2024, pp. 10734–10740.
[159] Z. Lin, W. Xin, J. Yang, Z. QingPei, and L. ZongJie, "Dynamic trajectory-tracking control method of robotic transcranial magnetic stimulation with end-effector gravity compensation based on force sensors," *Ind. Robot, Int. J.*, vol. 45, no. 6, pp. 722–731, Dec. 2018.
[160] M. Dominici and R. Cortesao, "Model predictive control architectures with force feedback for robotic-assisted beating heart surgery," in *Proc. IEEE Int. Conf. Robot. Autom. (ICRA)*, May 2014, pp. 2276–2282.
[161] Q. Ren, W. Zhu, Z. Feng, and W. Liang, "Learning-based force control of a surgical robot for tool-soft tissue interaction," *IEEE Robot. Autom. Lett.*, vol. 6, no. 4, pp. 6345–6352, Oct. 2021.
[162] L. Richter, G. Neumann, S. Oung, A. Schweikard, and P. Trillenberg, "Optimal coil orientation for transcranial magnetic stimulation," *PLoS ONE*, vol. 8, no. 4, Apr. 2013, Art. no. e60358.
[163] J. G. Grab, E. Zewdie, H. C. Kuo, A. Giuffre, and A. Kirton, "Robotic TMS mapping of motor cortex in the developing brain," *Brain Stimulation*, vol. 10, no. 2, p. 473, Mar. 2017.
[164] K. Biernacki, M.-H. Lin, and T. E. Baker, "Recovery of reward function in problematic substance users using a combination of robotics, electrophysiology, and TMS," *Int. J. Psychophysiol.*, vol. 158, pp. 288–298, Dec. 2020.
[165] J.-P. Lefaucheur and T. Picht, "The value of preoperative functional cortical mapping using navigated TMS," *Neurophysiologie Clinique/Clinical Neurophysiol.*, vol. 46, no. 2, pp. 125–133, Apr. 2016.
[166] D. Frey et al., "Navigated transcranial magnetic stimulation improves the treatment outcome in patients with brain tumors in motor eloquent locations," *Neuro-Oncol.*, vol. 16, no. 10, pp. 1365–1372, Oct. 2014.
[167] T. Picht, D. Frey, S. Thieme, S. Kliesch, and P. Vajkoczy, "Presurgical navigated TMS motor cortex mapping improves outcome in glioblastoma surgery: A controlled observational study," *J. Neuro-Oncol.*, vol. 126, no. 3, pp. 535–543, Feb. 2016.
[168] G. Raffa et al., "The role of navigated transcranial magnetic stimulation for surgery of motor-eloquent brain tumors: A systematic review and meta-analysis," *Clin. Neurol. Neurosurgery*, vol. 180, pp. 7–17, May 2019.
[169] M. Bikson et al., "Guidelines for TMS/tES clinical services and research through the COVID-19 pandemic," *Brain Stimulation*, vol. 13, no. 4, pp. 1124–1149, 2020.
[170] L. M. Koponen, S. M. Goetz, D. L. Tucci, and A. V. Peterchev, "Sound comparison of seven TMS coils at matched stimulation strength," *Brain Stimulation*, vol. 13, no. 3, pp. 873–880, May 2020.
[171] M. C. Romero, M. Davare, M. Armendariz, and P. Janssen, "Neural effects of transcranial magnetic stimulation at the single-cell level," *Nature Commun.*, vol. 10, no. 1, p. 2642, Jun. 2019.
[172] P. B. Fitzgerald, "Targeting repetitive transcranial magnetic stimulation in depression: Do we really know what we are stimulating and how best to do it?" *Brain Stimulation*, vol. 14, no. 3, pp. 730–736, May 2021.
[173] B. Passera, A. Chauvin, E. Raffin, T. Bougerol, O. David, and S. Harquel, "Exploring the spatial resolution of TMS-EEG coupling on the sensorimotor region," *NeuroImage*, vol. 259, Oct. 2022, Art. no. 119419.
[174] H. Wang et al., "Individualized and clinically friendly helmet-type coil positioning method (I-Helmet) for transcranial magnetic stimulation," *Brain Stimulation*, vol. 15, no. 5, pp. 1023–1025, Sep. 2022.
[175] M. Koehler, T. Kammer, and S. Goetz, "How coil misalignment and mispositioning in transcranial magnetic stimulation affect the stimulation strength at the target," *Clin. Neurophysiol.*, vol. 162, pp. 159–161, Jun. 2024.
[176] Q. Noirhomme, M. Ferrant, Y. Vandermeeren, E. Olivier, B. Macq, and O. Cuisenaire, "Registration and real-time visualization of transcranial magnetic stimulation with 3-D MR images," *IEEE Trans. Biomed. Eng.*, vol. 51, no. 11, pp. 1994–2005, Nov. 2004.
[177] L. Richter, R. Bruder, P. Trillenberg, and A. Schweikard, "Navigated and robotized transcranial magnetic stimulation based on 3D laser scans," in *Bildverarbeitung Für Die Medizin 2011*, H. Handels et al., Eds., Berlin, Germany: Springer, 2011, pp. 164–168.
[178] M. Dannhauer et al., "Electric field modeling in personalizing transcranial magnetic stimulation interventions," *Biol. Psychiatry*, vol. 95, no. 6, pp. 494–501, Mar. 2024.